AD_____

Award Number: W81XWH-08-1-0292

TITLE: Anibamine and its Analogues as Novel Anti-Prostate Cancer Agents

PRINCIPAL INVESTIGATOR: Yan Zhang, Ph.D.

CONTRACTING ORGANIZATION: Virginia Commonwealth University
Richmond, Virginia, 23284

REPORT DATE: June 2009

TYPE OF REPORT: Annual

PREPARED FOR: U.S. Army Medical Research and Materiel Command
Fort Detrick, Maryland 21702-5012

REPORT DOCUMENTATION PAGE

Form Approved
OMB No. 0704-0188

1. REPORT DATE *(DD-MM-YYYY)*	**2. REPORT TYPE**	**3. DATES COVERED** *(From - To)*
06/30/2009	Annual	06/01/2008 to 05/31/2009

4. TITLE AND SUBTITLE
Anibamine and its Analogues as Novel Anti-Prostate Cancer Agents

5a. CONTRACT NUMBER
W81XWH-08-1-0292

5b. GRANT NUMBER
PC073739

5c. PROGRAM ELEMENT NUMBER

6. AUTHOR(S)
Yan Zhang

Email: yzhang2@vcu.edu

5d. PROJECT NUMBER

5e. TASK NUMBER

5f. WORK UNIT NUMBER

7. PERFORMING ORGANIZATION NAME(S) AND ADDRESS(ES)

Virginia Commonwealth University
Richmond, Virginia 23284

8. PERFORMING ORGANIZATION REPORT NUMBER

9. SPONSORING / MONITORING AGENCY NAME(S) AND ADDRESS(ES)
US Army Medical Research and Material Command
Fort Detrick, MD 21702-5012

10. SPONSOR/MONITOR'S ACRONYM(S)

11. SPONSOR/MONITOR'S REPORT NUMBER(S)

12. DISTRIBUTION / AVAILABILITY STATEMENT
Approved for public release; distribution unlimited

13. SUPPLEMENTARY NOTES

14. ABSTRACT
None provided.

15. SUBJECT TERMS
Prostate cancer, anibamine, CCR5 antagonist

16. SECURITY CLASSIFICATION OF:			**17. LIMITATION OF ABSTRACT**	**18. NUMBER OF PAGES**	**19a. NAME OF RESPONSIBLE PERSON**
a. REPORT	**b. ABSTRACT**	**c. THIS PAGE**			USAMRMC
U	U	U	UU	33	**19b. TELEPHONE NUMBER** *(include area code)*

Standard Form 298 (Rev. 8-98)
Prescribed by ANSI Std. Z39.18

Table of Contents

Introduction

The long-term goal of this research project is to develop CCR5 antagonists with the structure feature of anibamine as novel anti prostate cancer agents. The tasks of this project include: 1. Chemical synthesis of the ligand designed as anibamine derivatives; 2. Radio-ligand competition binding assay to evaluate the binding affinity of the ligands synthesized; 3. Characterization of CCL5 and CCR5 expression in SV40T-immortalized human prostate epithelial cell lines of the same cellular lineage with varying tumorigenicity and metastatic capacity in vivo (P69, M2182, M2205 and M12); 4. Investigation of the impact of chemokine receptor CCR5 antagonist on prostate cancer cell growth and progression using M12, PC-3, DU-145 and LNCaP cell lines; 5. Molecular modeling study. In order to achieve these aims, we have first designed and synthesized a series of anibamine analogs based on "Deconstruction-Reconstruction-Elaboration" method. So far thirty-two novel ligands have been prepared as derivatives of anibamine for biological screening assays. Second, several progressive biological assays to evaluate the anti prostate cancer activity of the ligands have been set up and pursued. Primarily, a RANTES-binding inhibition assay protocol has been set up and ready to test our drug candidates. Additionally, biological screening includes the test of capacity of these novel compounds to inhibit proliferation and/or apoptosis by the human prostate cancer cell lines M12, PC-3, DU-145 and LNCaP has been conducted to evaluate their efficacy. Also we have assessed changes in the expression of CCL5 and CCR5 in human prostate epithelial cell lines of the same cellular lineage but with differing in vivo phenotypes (P69SV40TAg, M2182, M2205, and M12). A molecular modeling study has been conducted to elucidate the interaction of anibamine, the lead compound, to the target protein, chemokine receptor CCR5, to further facilitate our next generation molecular design. This part of work has been published in the Journal of Chemical Informatics and Modeling.

Annual Progress Report

The long-term goal of this research project is to develop CCR5 antagonist with the structure feature of anibamine as novel anti prostate cancer agents. Based on the approved Statement of Work of this award, the following tasks will be accomplished within two-year period of time:

Task 1. Chemical synthesis of the ligand designed as anibamine derivatives

Task 2. Radio-ligand competition binding assay to evaluate the binding affinity of the ligands synthesized

Task 3. Characterization of CCL5 and CCR5 expression in SV40T-immortalized human prostate epithelial cell lines of the same cellular lineage with varying tumorigenicity and metastatic capacity in vivo

Task 4. Investigation of the impact of chemokine receptor CCR5 antagonist on prostate cancer cell growth and progression using M12, PC-3, DU-145 and LNCaP cell lines

Task 5. Molecular modeling study

In the past one year all five tasks have pursued accordingly and the results are summarized below:

Task 1. Chemical synthesis of the ligand designed as anibamine derivatives

Our laboratory has accomplished the total synthesis of anibamine and published the results in *Organic Letters*, 2007, 9(10), 2043-6. This biosynthetic approach is being applied directly to our current chemical synthesis of the newly designed derivatives of anibamine. The initial structural modification of anibamine is following the "Deconstruction-Reconstruction-Elaboration" method, as proposed in Figure 1.

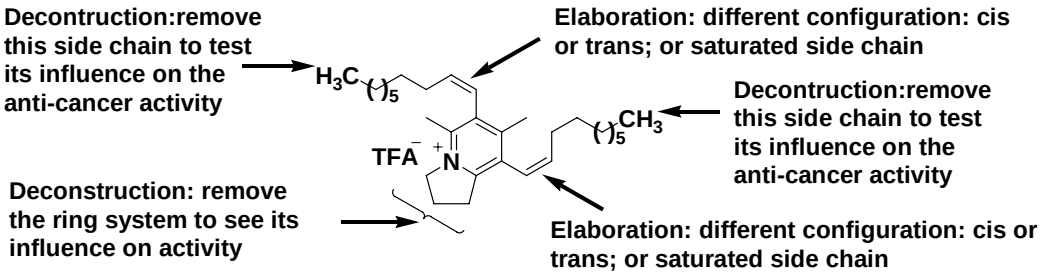

Figure 1. Initial structure modification of anibamine

1.1 Deconstruction procedure

1.1.1 Core ring system The central ring system of anibamine largely determines the molecular conformation of anibamine. Thus, by removing the fused ring, the conformation of the molecule will be changed. Shown in scheme 1, the synthesis of non-ring derivatives of anibamine was very straightforward. The methyl group was introduced with little difficulty.

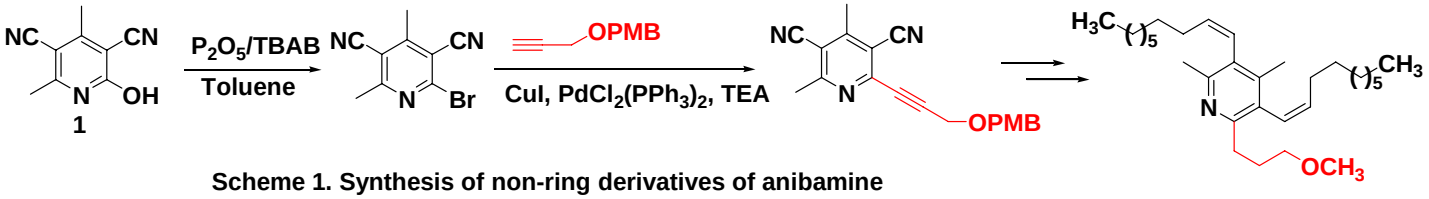

Scheme 1. Synthesis of non-ring derivatives of anibamine

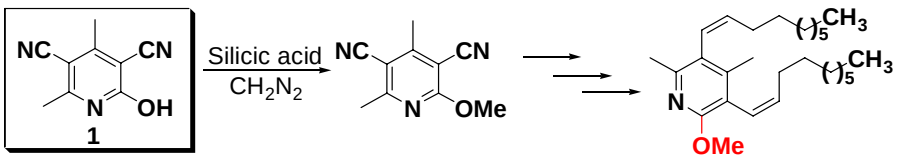

Scheme 2. The synthesis of anibamine derivative with non-fused-ring system

Another obvious modification is to remove the core ring system totally and test if that will influence the activity. The synthesis of the ligand was accomplished by following the routes in scheme 2.

1.1.2 Side chains Alternative removal of side chain at position 5 or 3 will test the influence of side chains to the anti prostate cancer activity of anibamine. The synthesis of these two compounds was finished by following scheme 3 and 4.

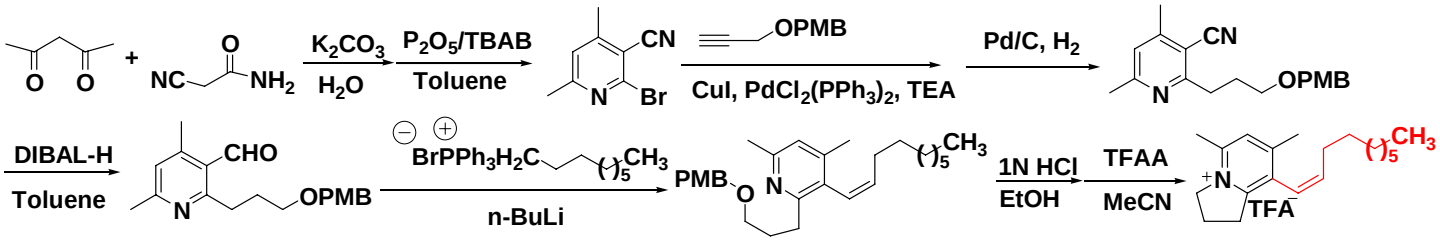

Scheme 3. Synthesis of one side chain at position-3 derivative of anibamine

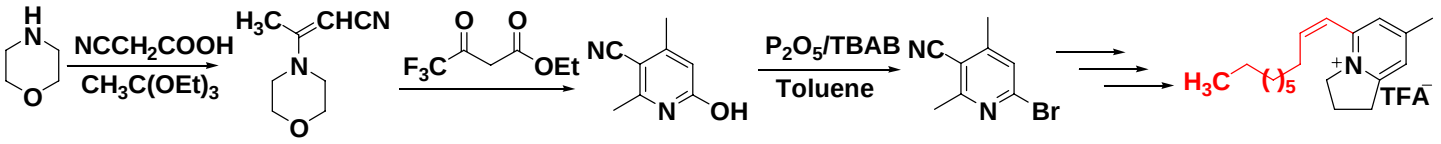

Scheme 4. The synthesis of one side chain at position 5 derivative of anibamine

1.2 Reconstruction procedure Based on the biological screening results (being conducted right now) of the deconstruction products (**1.1**), we will reconstruct the skeleton of the active molecules to verify the essential pharmacophore(s) in the parent compounds. Total of six compounds may be synthesized to verify their activity.

1.3 Elaboration procedure

1.3.1 Double bond configuration We further changed the double bond configuration from cis to trans in the molecule to test such elaboration's influence on the anti prostate cancer activity (Scheme 5).

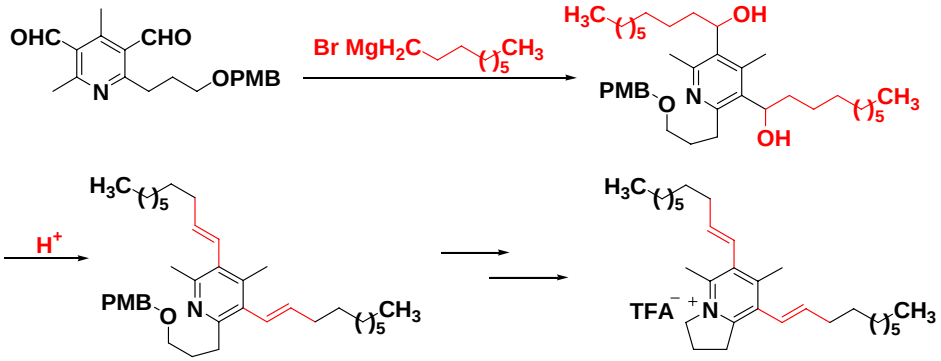

Scheme 5. Anibamine derivative synthesis with different double bond configuration

1.3.2 Core ring system modification By changing the size of the fused ring, the conformation of the molecule will be changed. This may change its binding affinity to CCR5 significantly and further influence their anti prostate cancer activity. As shown in scheme 6, the syntheses of ring-size modified derivatives of anibamine were straightforward.

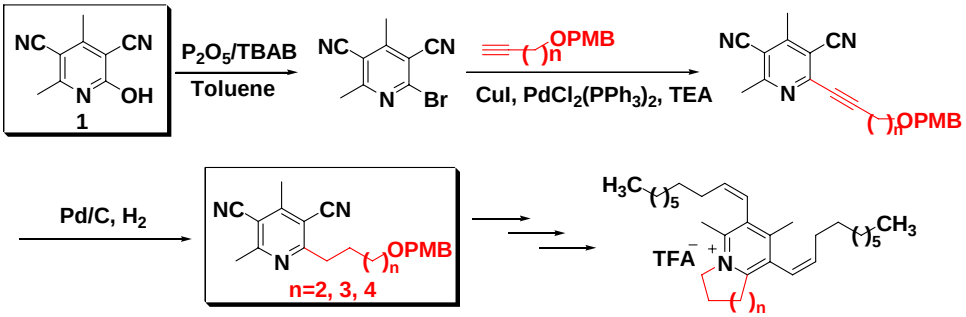

Scheme 6. Synthesis of ring system modified derivatives of anibamine

1.3.3 Side chain further modification Based on the fact that, first, the calculated log K_{ow} for anibamine is 9.1, which indicates that its lipophilicity is significant higher than the value set forth by "Lipinski's rule of 5" for drug-like compounds; second, in comparing the chemical structure of anibamine with other known CCR5

antagonists the major difference is that the two anibamine side chains are simple, undecorated, aliphatic chains, we decided to introduce more chemical structure features on these side chains that will effectively drive this structure-activity relationship study. We replaced the long aliphatic side chains with substituted benzene ring systems with the same or similar number of carbons. Some of the model compounds are listed in Table 1. The chemical synthesis of these compounds was conducted by following scheme 1, 3 and 4.

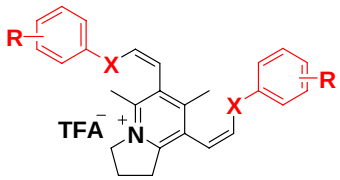

Table 1. Spacer and substitutions for the side chain modification

Spacer X	None, CH_2, CH_2CH_2
R (bulky effect)	OCH_3, OCH_2CH_3, O-i-Pr, O-c-pentyl, O-c-hexyl
R (electronic effect)	NH_2, OCH_3, CH_3, H, F, Cl, Br, NO_2, CF_3, SO_3Me

Among all the ligands described in Table 1, we have finished the synthesis of **twenty-four** compounds. We hope to be able to apply the biological screening results of these ligands to guide our choices in our side chain modification (up to forty-five novel ligands may be synthesized eventually).

In summary, total of **thirty-two** novel ligands as anibamine derivatives have designed and synthesized through multi-step chemical synthesis. They all have been fully characterized by NMR, IR, and MS. Elementary analysis were also conducted for each compound for final verification of their chemical composition.

Task 2. Radio-ligand competition binding assay to evaluate the binding affinity of the ligands synthesized

2.1 RANTES binding inhibition assay We have setup a radio-ligand binding assay protocol to conduct the RANTES binding inhibition assays to test the CCR5 receptor affinity of all the compounds synthesized. The assay is now being conducted for all the compounds so far synthesized.

To test the CCR5 receptor affinity of the compounds synthesized, Chinese hamster ovary (CHO) cells expressing human CCR5 will be used in the binding experiments. The experiment will be conducted at room temperature in the presence of [^{125}I]RANTES. IC_{50} values (the concentration required to inhibit the binding of [^{125}I]RANTES by 50%) will be used to evaluate the relative affinity of the compounds to CCR5. Normally, compounds with an IC_{50} concentration at 10μM or lower are considered active and will be further evaluated in additional in vitro assays. The binding assay will provide preliminary data for further molecular design, especially as guided by molecular modeling where downstream biological effects are not explicitly considered.

2.2 Protocol

2.2.1 CCR5/CHO Cell Transfection CHO Cells are transfected with CCR5 plasmid DNA (UMR cDNA Resource Center) using LipofectAMINE Reagent (GibcoBRL) according to the manufacturer's recommendation. Briefly, a lipid/DNA mixture is prepared in 200 µL of serum-free media (3 µL lipid and 1 µg DNA) and incubated for 45 min at 22°C. Serum-free media is then added to bring the final volume to 1 mL, which is then added to each well of cells. After 3 hr, the lipid/DNA mixture is removed and replaced with 1 mL of FBS-containing medium. For selection of stable cell lines, the media is replaced with selection media (containing 4 to 6 mg/mL of G418) after 36 hr. These cells are then split into 96 well plates at a concentration of 1 cell per three wells. The entire time the cell are being grown in the presence of 1 mg/mL of G418 to continue to maintain the selection process. Once the cells get confluent, Western blots will be conducted for each clone utilizing a human CCR5 polyclonal antibody. The cloned cells with CCR5 expression will be adopted to further cell culture.

2.2.2 Cell Culture and Drug Treatments Cells are cultured in a humidified atmosphere of 5% CO_2/95% air at 37°C. The medium is a 1:1 mixture of DMEM and Nutrient Mixture F12 containing 5% fetal bovine serum, 100 units/mL each of penicillin and streptomycin. Transfected cell medium also contains 0.4 mg/mL G-418.

2.2.3 Membrane Homogenate Preparation Cells are harvested by replacing the media with PBS + 0.4% EDTA and collected by centrifugation at 1000 x g. Samples are homogenized in 20 volumes ice-cold membrane buffer (50 mM Tris-HCl, 3 mM $MgCl_2$, 1 mM EGTA, pH 7.4) with a Polytron. The homogenate is centrifuged at 48,000 x g for 10 min, resuspended in assay buffer (50 mM Tris-HCl, 3 mM $MgCl_2$, 0.2 mM

EGTA, pH 7.4), centrifuged again as above, and resuspended in assay buffer. Protein values are determined by the Bradford method.

2.2.4 CCR5 Receptor Binding Saturation binding is performed by incubating membranes for 90 minutes at 30°C with 0.5-15 nM [^{125}I]RANTES in assay buffer in a 0.5 mL volume. Non-specific binding is determined with 200 nM RANTES. For competition assays, membranes are incubated as above with 2 nM [^{125}I]RANTES and various concentrations of unlabeled ligand, to determine competitor affinity for CCR5. The reaction is terminated by rapid filtration (GF-C filter paper is presoaked for at least half hour in 0.3% PEI solution). Bound radioactivity is determined by gamma counter for [^{125}I] immediately [54].

2.2.5 Data analysis For competition binding assay, linear regression analysis of Hill plots (plot of log[B / (B_0 - B)] as a function of log[X]; where B is the pmol/mg of radioligand bound and X is the concentration of unlabeled competitor) will be conducted to determine the IC_{50} value for each ligand. "B" will be calculated as % of radioligand bound at each concentration of competitor and B_0 will be normalized to be 100%. The IC_{50} values (inverse log X where B = 50%) will then be determined and corrected to K_i values using the Cheng-Prusoff equation: $K_i = IC_{50} / (1 + (L/K_D))$, where L is the concentration and K_D is the K_D value of the radioligand. All linear and non-linear curve-fitting analyses will be performed using Prism 4.0 software.

2.3 Results The binding assay is now being conducted under the supervision of Dr. Dana E. Selley of the Department of Pharmacology and Toxicology at Virginia Commonwealth University. Both the PI's lab and Dr. Selley's lab have fully functional binding assay facility. The assays will be pursued mainly in the PI's lab while Dr. Selley's lab will provide necessary technical support. The results will be summarized and reported in due course.

Task 3. Characterization of CCL5 and CCR5 expression in SV40T-immortalized human prostate epithelial cell lines of the same cellular lineage with varying tumorigenicity and metastatic capacity in vivo

SYBR-Based Real-time PCR: protocol and results

Gene expression of CCR5 and CCL5 was quantitated by SYBR-based Real-time PCR. The U6 gene was used as internal control. cDNA was synthesized using the iScript cDNA Synthesis Kit (Biorad) in a 20 μl reaction volume including 4 μl of iScript reaction mix, 1 μl of iScript reverse transcriptase and 1 μg of total RNA. The reactions were incubated first at 25°C for 5 min and then at 42°C for 30 min followed by inactivation at 85°C for 5 min. The CCL5, CCR5 and U6 genes were amplified by Real-time PCR in a 7900HT Sequence Detection System (Applied Biosystems). The 20-μl PCR mixture included 10 μl of the 2X Universal SYBR Master Mix (Applied Biosystems), 1 μl of primers (10 μM) and 3 μl of reverse transcription (RT) product. The reactions were incubated in a 96-well plate at 50°C for 2 min, 95°C for 10 min, followed by 40 cycles of 95°C for 15 s, 55°C for 35 s and 68°C for 35 s. Primers used for the CCL5 gene were 5'-CTCATTGCTACTGCCCTCTGCGCTCCTGC-3' and 5'-GCTCATCTCCAAAGAGTTGATGTACTC-3'. Primers used for CCR5 gene were 5'-TTGAGTCCGTGTCACAAGCCC-3' AND 5'-AATAATTGCAGTAGCTCTAACAGG-3' Primers used for U6 gene were 5'-CTCGCTTCGGCAGCACA-3' and 5'-AACGCTTCACGAATTTGCGT-3'. The threshold cycle (CT) was defined as the fractional cycle number at which the fluorescence passed the fixed threshold (0.2). The relative quantity (RQ) of the target miRNAs was estimated by the ΔΔCT study using U6 expression as an endogenous control for each reaction. Relative expression was calculated using the comparative CT method.

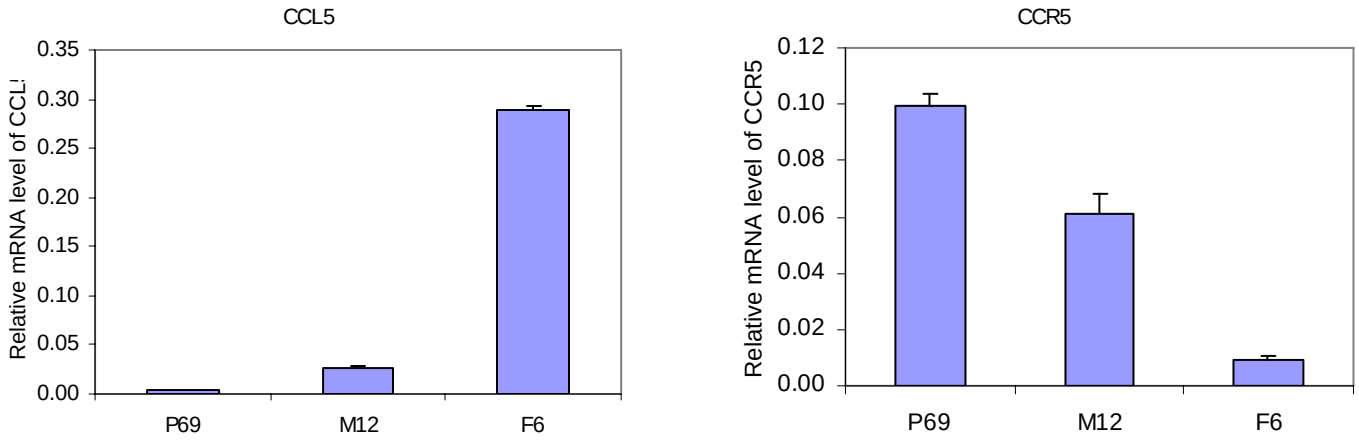

Figure 2. The qRT-PCR results to characterize the expression of CCL5 and CCR5 in different cell lines.

From Figure 2, it appears that the expression levels of CCL5 and CCR5 is correlated with the tumorigenicity and metastatic capacity of different cell lines. That is, the higher the tumorigenicity and metatstatic capacity the cell line carries, the higher the expression level of its chemokine receptor CCR5 would be. Further interpretation and verification of the results will be conducted after more prostate cancer cell lines would be examined.

Task 4. Investigation of the impact of chemokine receptor CCR5 ant agonist on prostate cancer cell growth and progression using M12, PC-3, DU-145 and LNCaP cell lines

4.1 Anti Proliferation Assays The capacity of each synthesized compounds to inhibit the proliferation of several prostate cancer cell lines will be tested primarily as the first biological assay to evaluate their anti cancer activity.

4.2 Protocol

All cell lines, P69, PC-3, DU-145 and M12, were incubated at 37 ºC in the presence of 5% CO2. RPMI 1640 serum free media (GIBCO Invitrogen) containing 1 % L-glutamine, 0.1 % ITS (insulin, 5µg/ml; transferrin, 5µg/ml; and selenium, 5 µg/ml; Collaborative Research, Bedford) and 0.1 % gentamicin was used to cultivate all cells.

The media for DU-145 and PC-3 cell lines also included 10 % fetal bovine serum (FBS). The serum containing media for the M12 and P69 cell lines contained 5 % FBS. While the DU-145, PC-3 and P69 cells were all originally plated in media containing serum, the M12 cells were originally plated in serum containing media and then the next day were plated in serum free media and 0.01 percent epidermal growth factor (EGF). B. Anti-Proliferation Drug Assays

The effect of compounds designed as CCR5 antagonists on various prostate cancer tumor cell lines was assessed utilizing WST-1 Cell Proliferation Reagent (Roche). Prostate cancer tumor cells (DU-145, PC-3, M12 and P69) were plated out into 96 well plates (BD Falcon, VWR) at a concentration of 2000 cells per well. For the purpose of this study all cells were plated in RPMI media (GIBCO Invitrogen) containing 10 % fetal bovine serum, 1 % L-glutamine, 0.1 % ITS and 0.1 % gentamicin. The cells were placed in a total volume of 100 microliters per well and incubated overnight at 37 ºC and 5% CO2. Various concentrations of drug were plated the following day, maintaining a final total well volume of 150 microliters per well. In wells containing only cells and media or just media, a volume of 50 milliliters of PBS was added to each well. All drugs were dissolved in a minimum amount of dimethysulfoxide (Sigma-Aldrich) and the further dissolution was conducted with PBS buffer (GIBCO Invitrogen). Once the drugs were plated they were allowed to incubate with the cells for 24 hours at 37 ºC and 5% CO2.The next day 10 microliters of WST-1 Cell Proliferation Reagent (Roche) was added to each well, and incubated at 37 ºC and 5% CO2 for 3 hours. The absorbance of each well was then measured using an EL 312e Microplate Bio-kinetics Reader (BIO-TEK Instruments).

Calculations of % inhibition and IC50 of each drug was performed utilizing a spreadsheet (Microsoft Office Excel 2007). The percent inhibition was calculated by subtracting the average absorbance of the cells in the presence of drug from the absorbance of the cells with just media and then this value was divided by the difference between the absorbance of the cells without the drug and the absorbance of the media, all of which were multiplied by one hundred. The equation is, percent inhibition = [(Acells – Adrug) / (Acells – Amedia)] x 100, where A is the absorbance, cells is wells growing cells with no drug, drug is cells growing in the presence of drug and media is just media in the absence of both cells and drug.

4.3 Results and Discussion So far, nine compounds have been evaluated fully in three prostate cancer cell lines (DU-145, PC-3, and M12) for three timelines (24 hours, 48 hours, and 72 hours) at a serious of concentration (from 1 nM to 10 uM). As indicated in Figure 3, the inhibition of proliferation effect varies significantly depending on the chemical structure of the ligands. This provides important Structure-Activity-Relationship information to direct us for the next step molecule design. Further evaluation for all other ligands (synthesized and being synthesized) will be conducted following the same protocol. Once a complete data available, Quantitative Structure Activity Relationship (QSAR) will be conducted to provide detailed information for the next step molecular design.

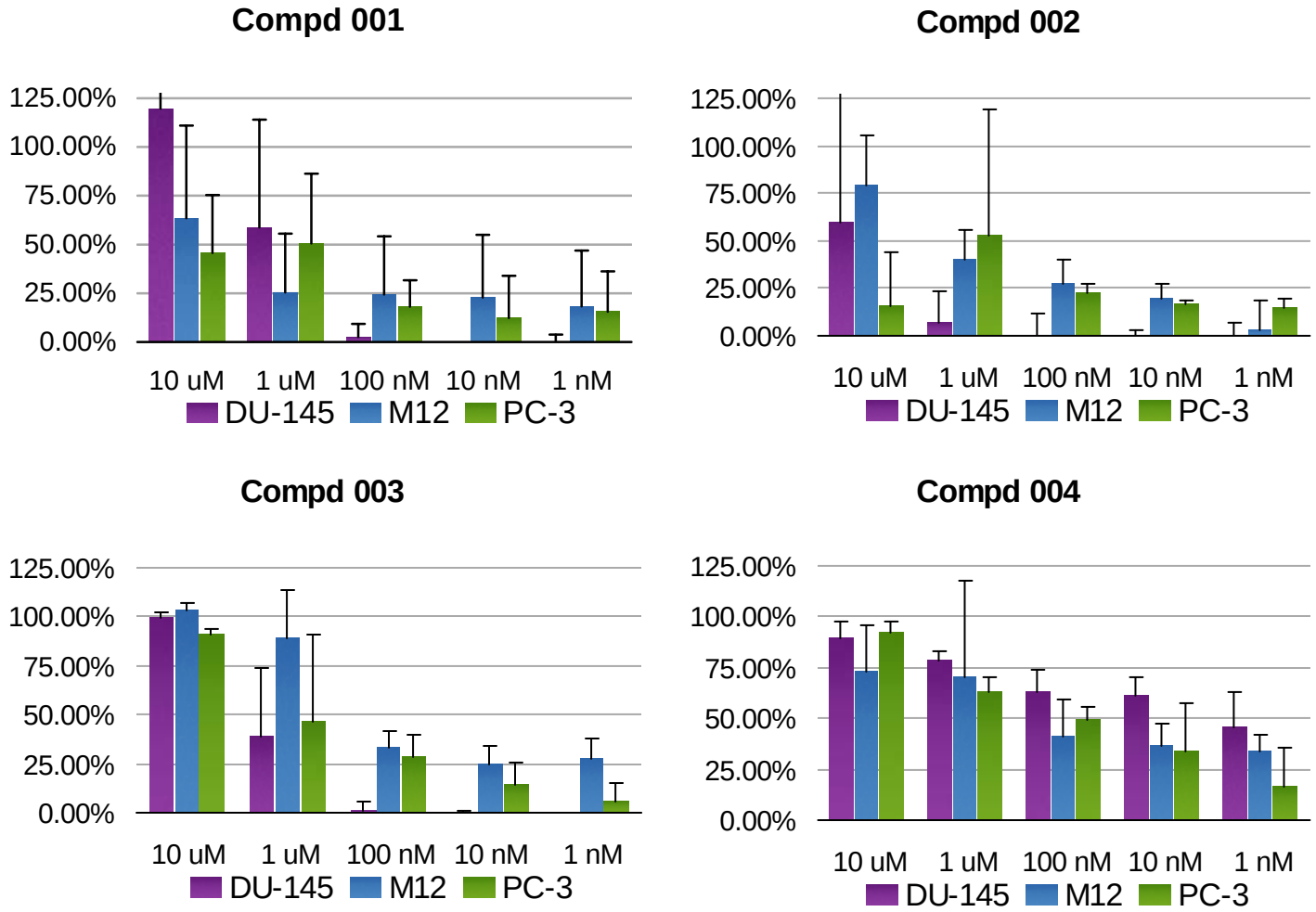

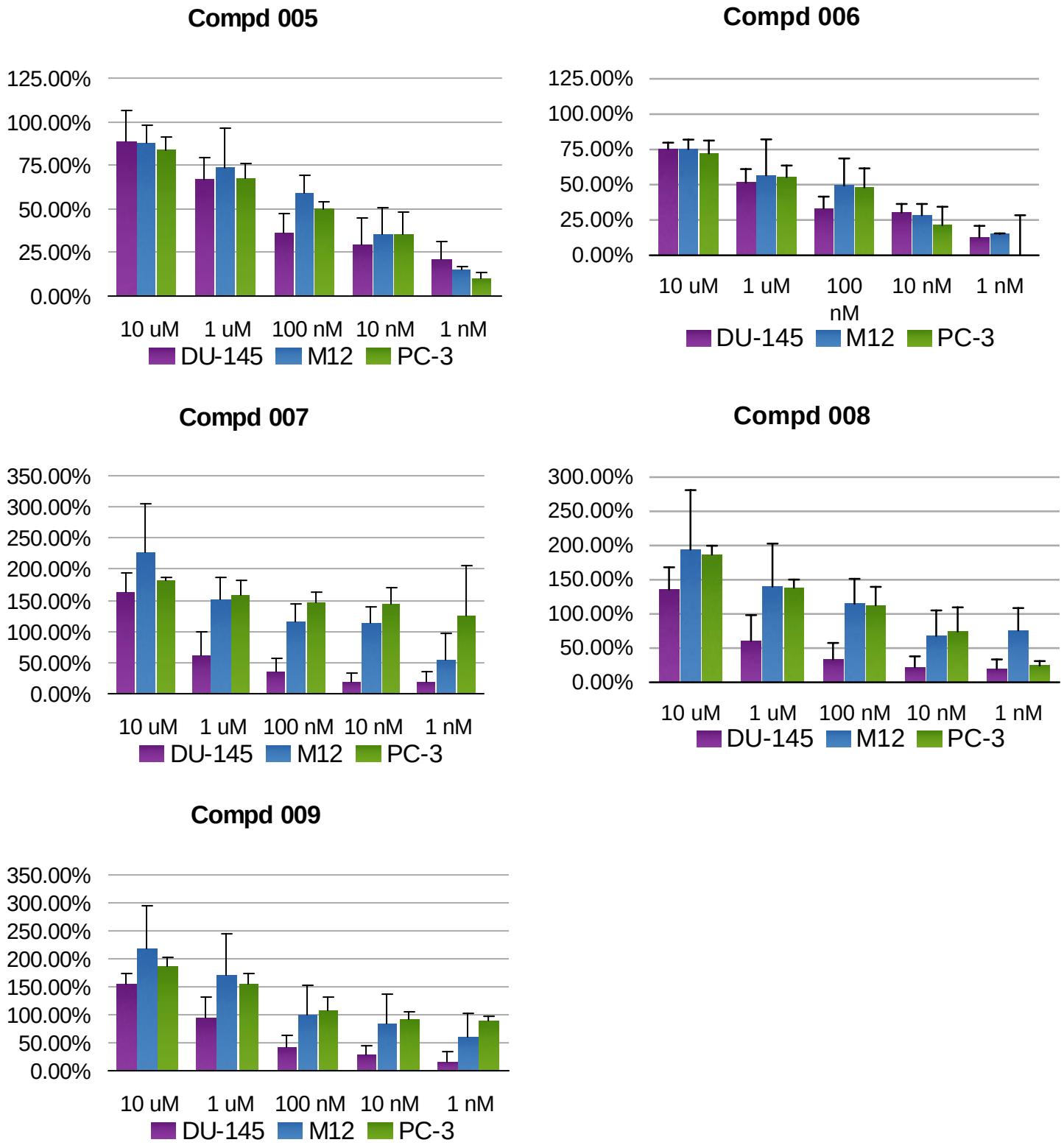

Figure 3. Inhibition effect of prostate cancer cell line proliferation by new ligands synthesized.

Task 5. Molecular modeling study

5.1. Homology modeling study of CCR5 receptor 3D model

As the first CCR5 natural product ligand, anibamine provides a novel structural skeleton that is remarkably different from all lead compounds previously identified as CCR5 antagonists. In order to characterize its interaction with the target protein, we conducted comparative docking studies of anibamine with several other known CCR5 antagonists in two CCR5 homology models built based on the crystal structures of bovine rhodopsin and human β_2-adrenergic receptor. From our study, the binding pocket of anibamine has some common features shared with other high affinity CCR5 antagonists, suggesting that they may bind in similar binding sites and/or modes. At the same time, several unique binding features of anibamine were identified and it will likely prove beneficial in future molecular design of novel CCR5 antagonists based on the anibamine scaffold. ***The part of research results have been published in the Journal of Chemical Informatics and Modeling, 2009, 49(1), 120-32.***

5.2 Small molecule construction For all the small molecules (designed and synthesized ligands), their conformation has been optimized after being constructed in Sybyl 7.0. They are ready for the next step molecular modeling study.

Key Research Accomplishments

- A series of novel ligands have been designed based on the chemical structure of anibamine, the first nature product chemokine receptor CCR5 antagonist.

- Chemical synthesis of thirty-two (32) novel ligands among this series has been finished and all the ligands have been characterized fully to verify their chemical structures.

- A RANTES binding inhibition assay has been set up and the protocol has been verified using RANTES and TAK-779. The method is ready for the screening of synthesized compounds.

- Gene expression of CCR5 and CCL5 was quantitated by SYBR-based Real-time PCR for three cell lines, P69, M12, and F6.

- Antiproliferation assay to evaluate the anti prostate cancer activity of the new ligands has been conducted for nine new ligands. Three different prostate cancer cell lines are adopted and the cells are treated for 24, 48, and 72 hours with varies concentrations of ligands tested. All the ligands tested showed significant antiproliferation activity.

- A homology modeling study has been conducted to characterize the 3D conformation of chemokine receptor CCR5 and its interaction with the lead compound, anibamine.

Reportable Outcomes

One manuscript has been published so far (see Appendices) and two more manuscripts are under preparation for publication.

Two poster presentations related to this project have been presented at National and International level symposiums. They are:

1. Joanna L. Adams, Guo Li, Amanda C. Richardson, Joy L. Ware, and **Yan Zhang**. Prostate Cancer Cell Line Proliferation Inhibited by Anibamine, a Natural Product CCR5 Antagonist. Summit on Systems Biology 2007, June 5-7, 2007, Richmond, Virginia.

2. Kendra Haney, Guo Li, John Bajacan, **Yan Zhang**. Natural Product Based Novel Anti-Prostate Cancer Drug Discovery. Massey Cancer Center Research Retreat, Virginia Commonwealth University, June 2008, Richmond, Virginia.

One patent application has been prepared and the provisional invention related will be filed in due course.

One Master Degree student (Joanna Adams) has graduated after finishing a research project related.

One Master Degree student (Kendra Haney) is expected to graduate in the Summer of 2009 upon the completion of thesis based on this project.

One Postdoctoral Associate has been trained under the support of this award and is ready to apply for industrial chemist position.

Conclusion

The major focus of the research project will be the syntheses of the ligands we designed as chemokine receptor CCR5 antagonists with novel structural feature(s) derived from anibamine, the first natural product as a CCR5 antagonist. The biological characterization of these ligands for anti prostate cancer activity is being conducted. Once biological test results are available, Structure-Activity-Relationship (SAR) analyses will be conducted to identify the structural features for the next generation lead compound(s). When enough data is available, 3D QSAR studies will be performed. Concomitantly, we will refine our already completed homology model for the CCR5 receptor in response to these data.

So far we have finished the chemical synthesis of thirty-two novel ligands that are designed based on "Deconstruction-Reconstruction-Elaboration" method. A RANTES-binding inhibition assay protocol has been set up and ready to test our drug candidates. Other biological screening includes the test of capacity of these novel compounds to inhibit proliferation and/or apoptosis by the human prostate cancer cell lines M12, PC-3, DU-145 and LNCaP has been conducted to evaluate their efficacy. Also we have assessed changes in the expression of CCL5 and CCR5 in human prostate epithelial cell lines of the same cellular lineage but with differing in vivo phenotypes (P69, F6, and M12). A molecular modeling study has been conducted to elucidate the interaction of anibamine, the lead compound, to the target protein, chemokine receptor CCR5, to further facilitate our next generation molecular design.

In the next year, we will focus on the structure modification/elaboration part of the proposal by introducing more varieties of substitutions at the two side chains by following the "Lipinski's rule of 5" for drug-like compounds. Further biological screening will start from radioligand binding assay, to in vitro anti prostate cancer tests. We wish to identify a promising lead compound with novel chemical and structural features as well as high therapeutic indices to serve our long-term goal in finding a potent anti prostate cancer agent.

The medical product expected from this project in long term is discovery of a novel and potent anti prostate cancer agent with new therapeutic index.

Appendices

Reprints

Guo Li, Karen Watson, Robert W. Buckheit and **Yan Zhang**. Total Synthesis of Anibamine, a Novel Natural Product as Chemokine Receptor CCR5 Antagonist. *Organic Letters, 2007, 9, 2043-2046*.

Guo Li, Kendra M. Haney, Glen E. Kellogg, **Yan Zhang**. A Comparative Docking Study of *Anibamine* as the First Natural Product CCR5 Antagonist in CCR5 Homology Models. *J. Chem. Inf. Model., 2009, 49(1), 120-32.*

ORGANIC LETTERS

2007
Vol. 9, No. 10
2043−2046

Total Synthesis of Anibamine, a Novel Natural Product as a Chemokine Receptor CCR5 Antagonist

Guo Li,[†] Karen Watson,[‡] Robert W. Buckheit,[‡] and Yan Zhang*,[†]

Department of Medicinal Chemistry, Virginia Commonwealth University, 410 North 12th Street, P.O. Box 980540, Richmond, Virginia 23298-0540, and ImQuest BioSciences, Inc., 7340 Executive Way, Suite R, Frederick, Maryland 21704

yzhang2@vcu.edu

Received March 27, 2007

ABSTRACT

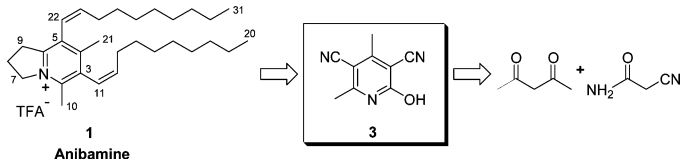

The total synthesis of anibamine, the first and only natural product known as a chemokine receptor CCR5 antagonist, is reported herein. Anibamine was synthesized from acetylacetone and cyanoacetamide in 10 steps.

Anibamine, a novel pyridine quaternary alkaloid recently isolated from *Aniba* sp.,[1,2] has been found to effectively bind to the chemokine receptor CCR5 with an IC_{50} at 1 μM in competition with ^{125}I-gp120, a HIV viral envelop protein binding to CCR5 with high affinity.[1] The chemokine receptor CCR5, a G-protein-coupled receptor, has been identified as an essential co-receptor for HIV virus entry to host cells.[3] Therefore, an antagonist of CCR5 receptor that would inhibit the cellular entry of human immunodeficiency virus type I (HIV-1) provides a new therapy choice for the treatment of HIV infection.[4]

Currently, all the known antagonists to CCR5 have been developed by optimization of the lead compounds from high-throughput screening, such as, SCH-D,[5] TAK220,[6] and UK427857[7] **(**Figure 1).

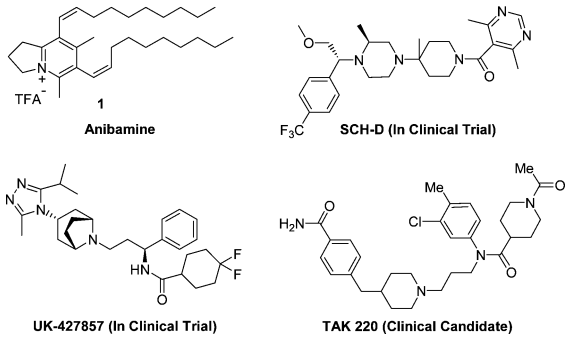

Figure 1. Anibamine and some known CCR5 antagonists

Anibamine is the first and the only natural product that has been identified as a CCR5 antagonist with high affinity.

* Address correspondence to this author.
[†] Virginia Commonwealth University.
[‡] ImQuest BioSciences, Inc.

(1) Jayasuriya, H.; Herath, K. B.; Ondeyka, J. G.; Polishook, J. D.; Bills, G. F.; Dombrowski, A. W.; Springer, M. S.; Siciliano, S.; Malkowitz, L.; Sanchez, M.; Guan, Z. Q.; Tiwari, S.; Stevenson, D. W.; Borris, R. P.; Singh, S. B. *J. Nat. Prod.* **2004**, *67*, 1036−1038.

(2) Klausmeyer, P.; Chmurny, G. N.; McCloud, T. G.; Tucker, K. D.; Shoemaker, R. H. *J. Nat. Prod.* **2004**, *67*, 1732−1735.

(3) (a) Samson, M.; Libert, F.; Doranz, B. J.; Rucker, J.; Liesnard, C.; Farber, C. M.; Saragosti, S.; Lapouméroulie, C.; Cognaux, J.; Forceille, C.; Muyldermans, G.; Verhofstede, C.; Burtonboy, G.; Georges, M.; Imai, T.; Rana, S.; Yi, Y.; Smyth, R. J.; Collman, R. J.; Doms, R. W.; Vassart, G.; Parmentier, M. *Nature* **1996**, *382*, 722−725. (b) Littman, D. R. *Cell* **1998**, *93*, 677−680.

(4) (a) Reeves, J. D.; Piefer, A. J. *Drugs* **2005**, *65*, 1747−1766. (b) Este, J. A. *Curr. Med. Chem.* **2003**, *10*, 1617−1632. (c) Schwarz, M. K.; Wells, T. N. C. *Nat. Rev. Drug Discovery* **2002**, *1*, 347−358. (d) Lusso, P. *EMBO J.* **2006**, *25*, 447−456.

10.1021/ol070748n CCC: $37.00
Published on Web 04/21/2007

Clearly, anibamine possesses a novel structural skeleton compared with all other known CCR5 antagonists.[5] Thus the chemical synthesis of anibamine and its analogues may lead to a new class of AIDS therapeutic agents. Herein is the first report of the total synthesis of anibamine.

As shown below, anibamine has a unique structural skeleton, in which a pyridine quaternary ion is embodied by a fused five-member ring. Such a skeleton can also be called the 2,3-dihydro-*1H*-indolizinium ion. On the pyridine ring, two ten-carbon aliphatic chains are attached at positions 3 and 5 via cis double bonds. In addition, both positions 2 and 4 are occupied by methyl groups. The retrosynthetic analysis of anibamine is illustrated in Scheme 1.

Scheme 1. The Retrosynthetic Analysis of Anibamine

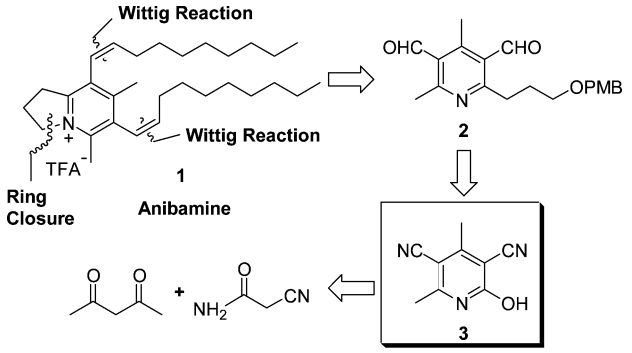

The two ten-carbon side chains can be introduced by Wittig reactions between the Wittig reagent of 1-bromononane and the 3,5-dialdehyde intermediate **2**. Intermediate **2** can be prepared by the reduction of the 3,5-dicyano intermediate. The fused five-member-ring system can be achieved by introducing a three-carbon side chain at position 2, followed by the cyclization reaction to form the indolizinium ring. Apparently the substituted pyridine **3** is the most critical intermediate since it possesses all the potential functional groups.

Two synthetic routes were explored to prepare the intermediate **3**, as shown in Scheme 2. In the first route, the condensation reaction between acetylacetone and *N*,*N*-dimethylformide dimethyl acetal provided compound **4**.[8] Then **4** was refluxed with hydroamine hydrochloride in methanol to give compound **5**.[9] Next **5** was coupled with aniline[10] to provide compound **6**. Finally the cyclization reaction between **6** and malononitrile[11] led to the intermediate **3** in an overall 30% yield. In the second route, using the

Scheme 2. The Chemical Synthesis of Intermediate **3**

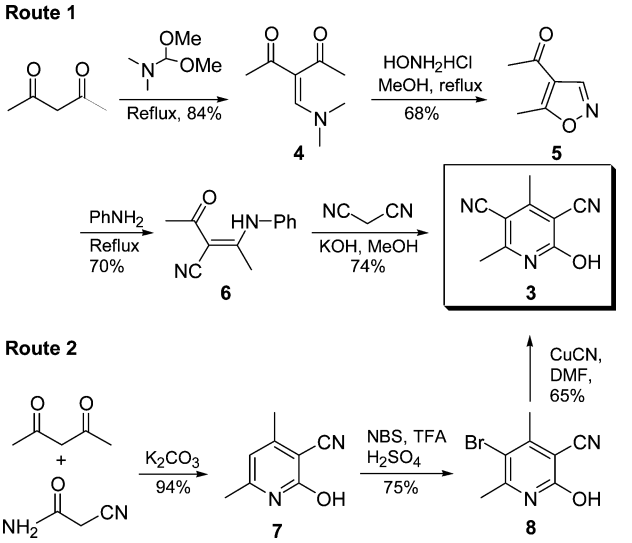

procedure of Haley et al.,[12] the condensation reaction between acetylacetone and cyanoacetamide gave compound **7**, which was brominated with NBS in TFA and H_2SO_4 to give **8**.[13] Next, the nucleophilic cyanization of compound **8** was achieved by refluxing with cuprous cyanide in DMF to give **3**.[13] Here, the total yield was 46% over 3 steps. The first route is one step longer than the second one, yet is more convenient for large-scale synthesis. Since two cyano groups can be introduced subsequently in the second route, it may provide the possibility of attaching two different side chains on positions 3 and 5. This will be critical to anibamine analogue synthesis in the future.

The bromination[14] of **3** with TBAB/P_2O_5 led to the 2-bromo-substituted intermediate **9** (Scheme 3). The pal-

Scheme 3. The Synthesis of Intermediate **11**

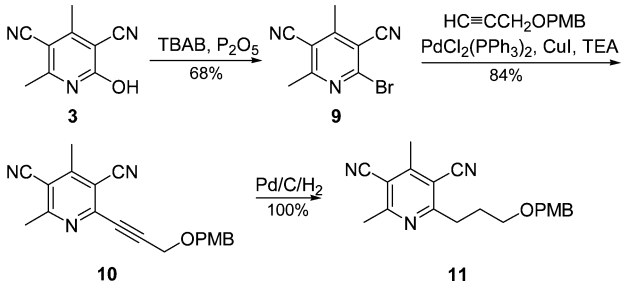

ladium-catalyzed alkynylation reaction of compound **9** with protected propargyl alcohol gave compound **10**.[15,16]

(5) Palani, A.; Tagat, J. R. *J. Med. Chem.* **2006**, *49*, 2851−2857.
(6) Imamura, S.; Ichikawa, T.; Nishikawa, Y.; Kanzaki, N.; Takashima, K.; Niwa, S.; Iizawa, Y.; Baba, M.; Sugihara, Y. *J. Med. Chem.* **2006**, *49*, 2784−2793.
(7) Wood, A.; Armour, D. *Prog. Med. Chem.* **2005**, *43*, 239−271.
(8) Schenone, P.; Mosti, L.; Menozzi, G. *J. Heterocycl. Chem.* **1982**, *19*, 1355−1361.
(9) Menozzi, G.; Schenone, P.; Mosti, L. *J. Heterocycl. Chem.* **1983**, *20*, 645−648.
(10) Alberola, A.; Antolin, L. F.; Gonzalez, M. A.; Pulido, F. J. *J. Heterocycl. Chem.* **1986**, *23*, 1035−1038.
(11) Alberola, A.; Antolin, L. F.; Gonzalez, M. A.; Laguna, M. A.; Pulido, F. J. *Heterocycles.* **1987**, *25*, 393−397.
(12) Haley, C. A. C.; Maitland, M. *J. Chem. Soc.* **1951**, 3155−3174.
(13) Mal, P.; Lourderaj, U.; Parveen; Venugopalan, P.; Moorthy, N. J.; Sathyamurthy, N. *J. Org. Chem.* **2003**, *68*, 3446−3453.
(14) Kato, Y.; Okada, S.; Tomimoto, K.; Mase, T. *Tetrahedron Lett.* **2001**, *42*, 4849−4851.
(15) Lautens, M.; Yoshida, M. *J. Org. Chem.* **2003**, *68*, 762−769.
(16) Negishi, E.; Anastasia, L. *Chem. Rev.* **2003**, *103*, 1979−2017.

To our delight, the hydrogenation of compound **10** under Pd/C in methanol at room temperature gave intermediate **11** in quantitative yield. After that, several different reducing agents were applied to prepare intermediate **2**. These results are summarized in Table 1.

Table 1. Preparation of Intermediate **2**

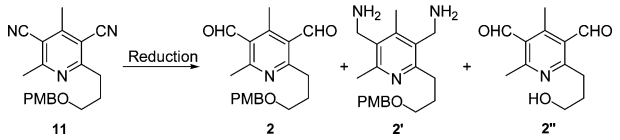

entry	reduction condition	product	yield (%)
1	Raney-Ni, NaH_2PO_2, Py/AcOH/H_2O	no reaction	
2	Raney-Ni, NaH_2PO_2, AcOH/H_2O	**2′**	70
3	Raney-Ni, 5 bar of H_2, AcOH	**2′**	95
4	Raney-Ni, 1 bar of H_2, AcOH	**2′**	90
5	Raney-Ni, 75% HCOOH aq	**2″**	13
6	DIBAL-H, THF, 0 °C to reflux	no reaction	
7	**DIBAL-H, toluene, 0 °C**	**2**	**77**

With use of Raney-Ni[17,18] as the reduction reagent in different solvent systems, the 3,5-diaminomethyl-substituted product (**2′**) was the only one except for the procedure with HCOOH as solvent, which led to compound **2″** in 13% yield. When DIBAL-H was used as the reduction reagent in toluene, the desired product (**2**) was obtained in 77% separation yield,[19] in contrast to the unsuccessful reaction in THF. Our explanation of this result is that the activity of the electrophilic reduction reagent DIBAL-H in toluene is higher than that in the comparatively more polar solvent THF.[20,21]

To introduce the aliphatic side chains onto positions 3 and 5, the Wittig reaction was explored under different basic conditions, such as NaH/toluene,[22] NaH/DMSO,[23] LHMDS,[24] and *n*-BuLi.[25] No reaction was observed when NaH was used as the base in toluene. A trace amount of the target product was observed while most of the starting material decomposed under NaH/DMSO and *n*-BuLi conditions. Finally, intermediate **12** was obtained as the major product when LHMDS was adopted as the base. We noticed that the crude dialdehyde **2** can be used in this step without further purification after the DIBAL-H reduction reaction, and the combined yield was 71% over two steps from compound **11**.

All four possible isomers were observed as products of this reaction (Scheme 4). Various chromatographic conditions have been applied yet no successful separation of any one of these four isomers has occurred. Therefore, after primary purification, the mixture was used for the next step. By calculating the ratios of the integrates of the methyl group at position 6 on the pyridine ring in the ^{1}H NMR spectrum, the composition of these four isomers in the mixture were determined, and compound **12** was characterized as the major one.

Scheme 4. The Wittig Reaction

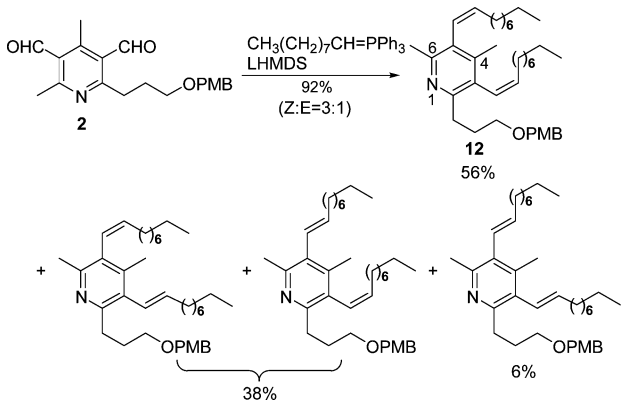

Interestingly, the most common PMB deprotection reagent, DDQ, was proved inefficient in both CH_2Cl_2/H_2O[26,27] and CH_2Cl_2/ buffer (pH 7) system[28] for compound **12**. In fact, the PMB group was removed quickly with reasonable yield under acidic conditions to give compound **13**.[29]

The five-member-ring closure was achieved by treating compound **13** with methanesulfonyl chloride and triethylamine at room temperature.[30,31] The crude product was purified by preparative HPLC with the previously reported condition.[1] Both anibamine (**1**) and its (11*E*,22*E*) isomer were isolated as the trifluoroacetic acid salts. The spectral properties of anibamine were compared with those in the literature and no significant differences were observed.

Scheme 5. The Synthesis of Anibamine

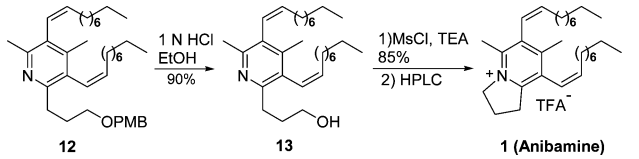

The anti-HIV activity of anibamine and its (11*E*,22*E*) isomer was evaluated. In an assay that determines inhibition

(17) Rapold, T.; Senn, M. U.S. Patent, 5,384,403, 1995.
(18) Heffner, R. J.; Jiang, J. J.; JoulliG, M. M. *J. Am. Chem. Soc.* **1992**, *114*, 10181−10189.
(19) Song, Z. J.; Zhao, M.; Desmand, R.; Devine, P.; Tschaen, D. M.; Tillyer, R.; Frey, L.; Heid, R.; Xu, F.; Foster, B.; Li, J.; Reamer, R.; Volante, R.; Grabowski, E. J. J.; Dolling, U. H.; Reider, P. J. *J. Org. Chem.* **1999**, *64*, 9658−9667.
(20) Bajwa, N.; Jennings, M. P. *J. Org. Chem.* **2006**, *71*, 3646−3649.
(21) Paquette, L. A.; Zhao, M. *J. Am. Chem. Soc.* **1993**, *115*, 355−356.
(22) Wightman, R. H.; Cresp, T. M.; Franz, S. *J. Am. Chem. Soc.* **1976**, *98*, 6052−6053.
(23) Kato, K.; Ohkawa, S.; Terao, S.; Terashita, Z.; Nishikawai, K. *J. Med. Chem.* **1985**, *28*, 287−294.
(24) Kan, T.; Fujiwara, A.; Kobayashi, H.; Fukuyama, T. *Tetrahedron* **2002**, *58*, 6267−6276.
(25) (a) Kiær, A.; Kjær, D.; Skrydstrup, T. *Tetrahedron* **1986**, *42*, 1439−1448. (b) Heathcock, C. H.; Finkelstein, B. L; Jarvi, E. T.; Radel, P. A.; Hadley, C. R. *J. Org. Chem.* **1988**, *53*, 1922−1942.

of HIV-1_{BaL} attachment to GHOST R5 cells, anibamine showed an EC_{50} at 0.6 μM and its (11*E*,22*E*) isomer did at 0.8 μM.[32]

In summary, anibamine was synthesized from acetylacetone and cyanoacetamide in 10 steps with 7.9% overall yield, or from acetylacetone and *N*,*N*-dimethylformide dimethyl acetal in 11 steps with 5.1% overall yield. To our knowledge, this is the first report of the total synthesis of anibamine. The above synthetic routes also offer the opportunity to prepare anibamine analogues for further biological evaluation and SAR study for their anti-HIV activity.

(26) Oikawa, Y.; Yoshioka, T.;Yonemitsu, O. *Tetrahedron Lett.* **1982**, *23*, 885−888.
(27) Horita, K.; Yoshioka, T.; Tanaka, T.; Oikawa, Y.; Yonemitsu, O. *Tetrahedron* **1986**, *42*, 3021−3028.
(28) Yu, W. S.; Zhang, Y.; Jin, Z. D. *Org. Lett.* ***2001***, *3*, 1447−1450.
(29) Jenkins, D. J.; Riley, A. M.; Potter, B. V. L. *J. Org. Chem*. **1996**, *61*, 7719−7726.
(30) Ciufolini, M. A.; Roschangar, F. *J. Am. Chem. Soc.* **1996**, *118*, 12082−12089.
(31) Bates, R. W.; Boonsombat, J. *J. Chem. Soc., Perkin Trans.* **2001**, *1*, 654−656.
(32) Dextran sulfate were provided as a relevant positive control compound for the individual assays, with anti-HIV activity of EC_{50} at 14.5 μM.

Acknowledgment. The project was partially supported by DHHS AI069975.

Supporting Information Available: Experimental procedures and spectroscopic data for all new compounds. This material is available free of charge via the Internet at http://pubs.acs.org.

OL070748N

Comparative Docking Study of Anibamine as the First Natural Product CCR5 Antagonist in CCR5 Homology Models

Guo Li, Kendra M. Haney, Glen E. Kellogg, and Yan Zhang*

Department of Medicinal Chemistry, School of Pharmacy, Virginia Commonwealth University, Richmond, Virginia 23298-0540

Received September 29, 2008

Anibamine, a novel pyridine quaternary alkaloid recently isolated from *Aniba sp*., has been found to effectively bind to the chemokine receptor CCR5 with an IC_{50} at 1 μM in competition with ^{125}I-gp120, an HIV viral envelope protein binding to CCR5 with high affinity. Since CCR5, a G-protein-coupled receptor, is an essential coreceptor for the human immunodeficiency virus type I (HIV-1) entry to host cells, a CCR5 antagonist that inhibits the cellular entry of HIV-1 provides a new therapy choice for the treatment of HIV. Anibamine provides a novel structural skeleton that is remarkably different from all lead compounds previously identified as CCR5 antagonists. Here, we report comparative docking studies of anibamine with several other known CCR5 antagonists in two CCR5 homology models built based on the crystal structures of bovine rhodopsin and human β_2-adrenergic receptor. The binding pocket of anibamine has some common features shared with other high affinity CCR5 antagonists, suggesting that they may bind in similar binding sites and/or modes. At the same time, several unique binding features of anibamine were identified, and it will likely prove beneficial in future molecular design of novel CCR5 antagonists based on the anibamine scaffold.

INTRODUCTION

According to UNAIDS Report 2006,[1] an estimated 38.6 million people worldwide were living with HIV at the end of 2005. In the United States about one million people are currently living with HIV.[2] Since the AIDS pandemic remains one of the leading global public health threats, the continued discovery and development of new antiretroviral drugs with reduced toxicity, enhanced potency, novel mechanisms of action, and reduced prevalence of adverse drug-drug interactions remains a very high priority. The chemokine receptors CCR5 and CXCR4 are essential coreceptors required for the attachment of HIV-1 to the host cell membrane[3−5] suggesting that CCR5 antagonists may lead to a novel therapeutic strategy in blocking the entry of HIV into host cells, especially when utilized in combination with the classical reverse transcriptase and protease inhibitors.[6,7] At the same time, the CCR5-Δ32 homo- and heterozygous genotype carriers have been shown to confer either resistance to HIV-1 infection or delayed progression of the disease.[8,9] Therefore, it is clear that CCR5 plays an essential role in HIV pathogenesis.

The chemokine receptor CCR5 (Figure 1) belongs to the extensively exploited family of G-protein-coupled receptors (GPCRs). Chemokines and chemokine receptors play a crucial role in the trafficking of leukocyte populations in the body and are involved in the development of a wide variety of human diseases.[10] Despite the fact that it has been more than ten years since the chemokine receptor CCR5 was identified as one of the essential coreceptors utilized by HIV-1 for entry into human CD4+ cells,[3−5] there are currently only a few CCR5 antagonists (Figure 2) being investigated as anti-HIV-1 agents in human clinical trials.[11−14] In fact, only one drug (Maraviroc or Selzentry) was approved by the FDA on August 6, 2007[14d] even though the FDA raised concerns that Maraviroc could be associated with an increased risk of liver damage, lymphoma, infections, and increased risk of heart attack.[14c,d] Also, clinical trials of Aplaviroc were halted due to severe liver side effects in both treatment-naive and treatment-experienced patients.[13b] It should be noted that the lead compounds for all of these CCR5 antagonists were discovered through high-throughput screening campaigns targeting the disruption of the virus attachment to the coreceptor. While this is often a valid approach that yields interesting lead compounds, natural products can often be more diverse, having novel structure skeletons with wider ranges of chemical shape and structural features. It is well-known[15] that natural products offer unmatched structural variety compared with combinatorial chemistry libraries, and their high diversity and specific biological activities very often make them useful resources for drug discovery.

Recently, anibamine, a novel pyridine quaternary alkaloid that was isolated from *Aniba sp.*, has been found to effectively bind to CCR5 with an IC_{50} of 1 μM in competitive binding assays with ^{125}I-gp120, a viral envelope protein that binds to CCR5 with high affinity.[16] As the first and only natural product to date showing CCR5 antagonism, anibamine has a novel structure quite different from those other known classes of CCR5 antagonists. Recently, we reported the total synthesis of anibamine[17] applying a flexible synthetic scheme that will allow the production of a wide variety of analogs.

It should be noted that the 1 μM activity of anibamine is in line with those of other "lead" compounds (0.39−2 μM)

* Corresponding author e-mail: yzhang2@vcu.edu.

10.1021/ci800356a CCC: $40.75
Published on Web 01/05/2009

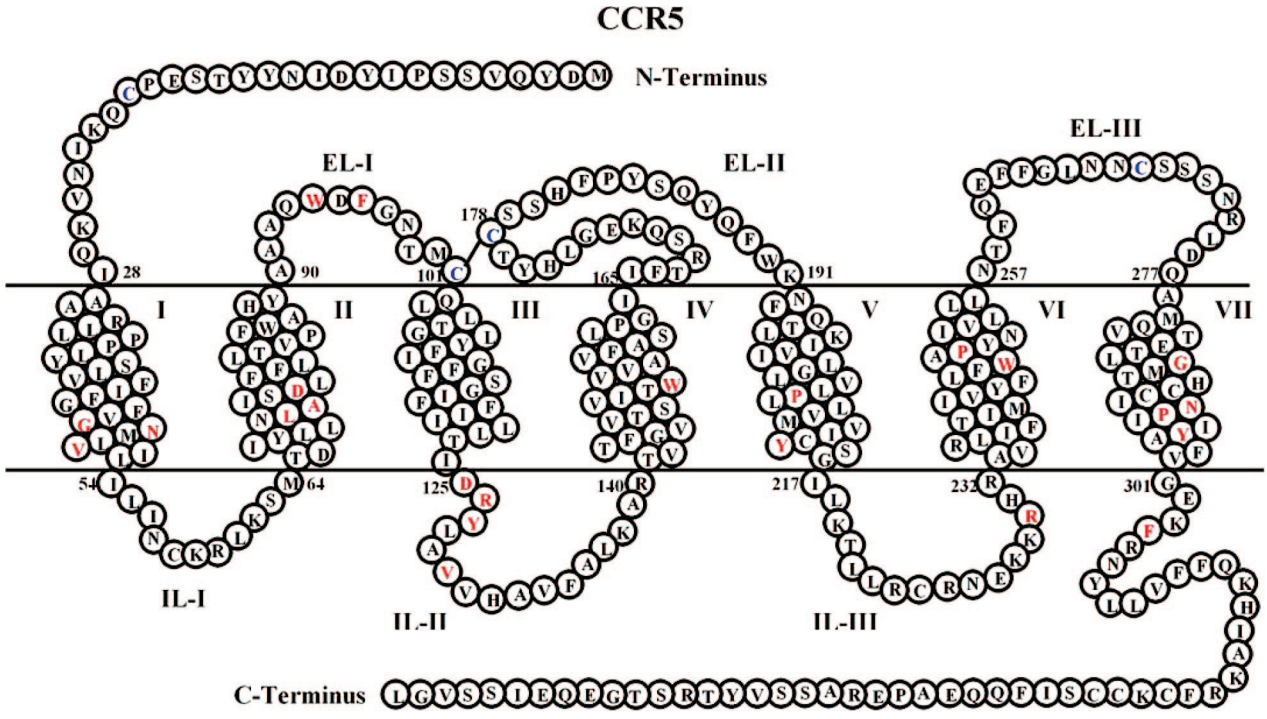

Figure 1. The schematic representation of the CCR5 sequence: EL, extracellular loop; IL, intracellular loop; I−VII, transmembrane helices.

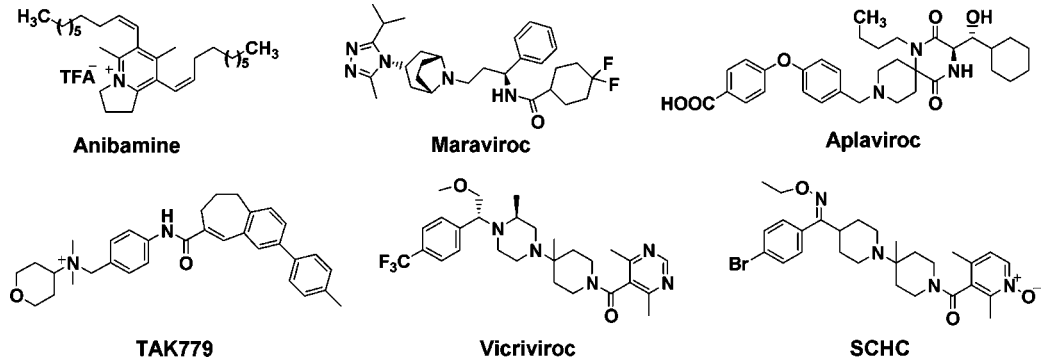

Figure 2. Chemical structures of anibamine and several known potential CCR5 antagonists.

that were developed into the antagonists illustrated in Figure 2.[17−21] Anibamine also has structural similarities to these compounds, in particular a potentially charged nitrogenic central moiety with two or more hydrophobic side chains attached. However, because of its structural novelty, we cannot dismiss the possibility that anibamine may possess a different binding modality than that proposed for the other CCR5 antagonists.[22] In the absence of experimental structural data for the CCR5 receptor, one of the few ways to investigate the binding modes of these compounds is through molecular modeling. An understanding of anibamine and its binding mode in CCR5 may assist the design of novel derivatives that are CCR5 antagonists with higher affinity. Since anibamine has a unique chemical structural skeleton with a potentially novel molecular design template, comparing its binding modality with those of other known CCR5 antagonists should be instructive regarding its activity and further validate it as a lead compound for next generation molecular design.

In general, computational and mathematical approaches, such as structural bioinformatics,[23] molecular docking,[24] molecular packing,[25] pharmacophore modeling,[26] Monte Carlo simulated annealing approach,[27] graph/diagram approach,[28] diffusion-controlled reaction simulation,[29] biomacromolecular internal collective motion simulation,[30] QSAR,[31] protein subcellular location prediction,[32] identification of membrane proteins and their types,[33] identification of enzymes and their functional classes,[34] identification of GPCR and their types,[35] identification of proteases and their types,[36] protein cleavage site prediction,[37] and signal peptide prediction[38] can provide useful information and insights for both basic research and drug design and hence are widely welcome by the science community.

More specifically, in the absence of specific structural data, molecular modeling studies that build and refine homology models of the receptor and dock the various ligands into these models are the most accessible approaches to studying binding modes for ligands. Like nearly all GPCRs, a crystal structure for the CCR5 receptor is not currently available, and a template-derived homology model has to be used to gain insight into the receptor structure. In fact, a homology modeling method based on the crystal structure of bovine rhodopsin[39] has been successfully applied to other GPCRs,[40] including the CCR5 receptor,[22] to further understand the

ligand-protein interactions and to identify new and potent ligands. For example, a homology model of Angiotensin II type 1 (AT1) receptor was used to explore the binding sites of several nonpeptide AT1 receptor antagonists,[41] and a homology model of M1 muscarinic acetylcholine receptor was applied to understand the mechanism by which the agonist-receptor complex activates the G proteins.[42] More relevant, the models of CCR5 developed by several groups helped characterize the binding mode of known CCR5 agonists and antagonists.[22] It is believed that with all the lessons learned from previous experience, homology modeling of GPCRs based on bovine rhodopsin crystal structure will help in structure-based drug design and virtual screening for therapeutic applications at many GPCR targets. The recent seminal resolution of two human β_2-adrenergic receptor (β_2AR) crystal structures[43] led us to question which crystal structure would be the more reasonable template for building the homology model of the CCR5 receptor. Both β_2AR structures have a bound inverse agonist carazolol, and presumably these structures were closer to the inactive state of β_2AR. However, the broken ionic locks in the reported structures and the increased affinity of β_2AR-T4 chimera for agonists compared to the wild type β_2AR suggest that these β_2AR crystal structures seemed closer to the active state of the β_2AR receptor or, possibly, a state between active and inactive.[44] Thus, a homology model based on the β_2AR structure would also be worth exploring for valuable information of CCR5 receptor.

In this study, the binding mode of anibamine in the antagonist locus of CCR5 has been studied by building and analyzing two complete (i.e., including both the extracellular and intracellular loops) homology models of the CCR5 receptor. As in nearly all homology models of GPCRs, one of our models was based on the crystal structure of bovine rhodopsin in the dark state (PDB code 1F88), which was, up until very recently, the only available crystal structure for a GPCR. The other homology model was constructed based on the crystal structure of β_2AR (PDB code 2RH1). The docking studies of known CCR5 antagonists into each of these two CCR5 homology models showed that the CCR5 homology model based on the bovine rhodopsin crystal structure seemed more compatible with the site-directed mutagenesis study results. The docking studies of anibamine in these two homology models showed that the anibamine binding mode shares some common binding features with other CCR5 antagonists. Interestingly, some unique intermolecular interactions between anibamine and the CCR5 receptor homology model may further direct structural modifications of anibamine as a lead for next generation CCR5 antagonist design.

RESULTS AND DISCUSSION

The computational analysis of anibamine was processed in several steps: first, we performed a conformational study of it and other known CCR5 antagonists. Next, homology models of the chemokine receptor CCR5, including transmembrane, extracellular and intracellular components, were built based on the crystal structure of bovine rhodopsin and human β_2AR, followed by molecular dynamics simulation/annealing to optimize the conformations of the models. Finally, anibamine and the other ligands were docked into these two CCR5 models, with particular emphasis on evaluating the CCR5 binding pocket interactions with anibamine and other known CCR5 antagonists.

Conformation Study of Anibamine and Other Known CCR5 Antagonists. In order to simulate the conformation of anibamine in a biological system as well as in the CCR5 binding site, a conformation study was conducted by minimization and molecular dynamics simulations. Other compounds reported to be potential CCR5 antagonists, including Aplaviroc, Maraviroc, and Vicriviroc that have entered clinical trials, were similarly analyzed. The lowest energy conformation obtained for each ligand was further simulated in a solvated system, and these results were then applied to the initial conformation to explore their binding modes in the CCR5 receptor antagonist binding locus. These conformations were only expected to provide a reasonable starting point for our docking studies; they were to endure some possibly dramatic alterations during docking in order to achieve the lowest energy conformations for the ligand−receptor complex (vide infra).

Homology Modeling of Chemokine Receptor CCR5. Chemokine receptors belong to the rhodopsin subfamily in the GPCR superfamily and are characterized by a heptapeptidic transmembrane helical fold (7-TM) spanning the plasma membrane (see Figure 1). Homology modeling studies of the CCR5 receptor, based on the crystal structures of the dark state bovine rhodopsin at 2.8 Å resolution (PDB code 1F88)[39b] and on the human β_2AR structure at 2.4 Å resolution (PDB code 2RH1),[43a] involved several steps: sequence alignment, assignment of Cartesian coordinates for amino acid residues in structurally conserved regions, assignment of coordinates for amino acid residues in structurally nonconserved regions, and refinement of coordinates of side chains of the entire protein.

The initial, and likely most essential, step in homology modeling is sequence alignment among the CCR5, the bovine rhodopsin, and the human β_2AR. This was performed for the entire protein sequences by using the InsightII/Homology module (Figure 3). In order to confirm the alignment automatically generated by the software, manual alignment of the amino acid residues was also performed by comparing the chemical structures of the autoaligned residues. While the entire protein sequences homology level was approximately 20% among all three proteins, their transmembrane domains gave 58% homology identity between the bovine rhodopsin and CCR5 while 56% between human β_2AR and CCR5 (Table 1). This further validated applying these two crystal structures as templates to construct homology models of the CCR5 receptor. It is important to note that CCR5 receptor's sequence contains all of the conserved amino acid residues found in most GPCRs, and this provides an important guideline for sequence alignment.

The overlapping amino acid sequences between rhodopsin, β_2AR, and the CCR5 receptor, i.e., structurally conserved regions, were divided into different lengths separated by gaps (most of which are in the loop domains). The coordinates for the amino acid residues in these regions of rhodopsin or β_2AR were assigned to the corresponding residues in the CCR5 receptor.

The remaining amino acid residues of the CCR5 receptor constitute the structurally nonconserved regions, while most of them are in the extracellular and intracellular loop regions.

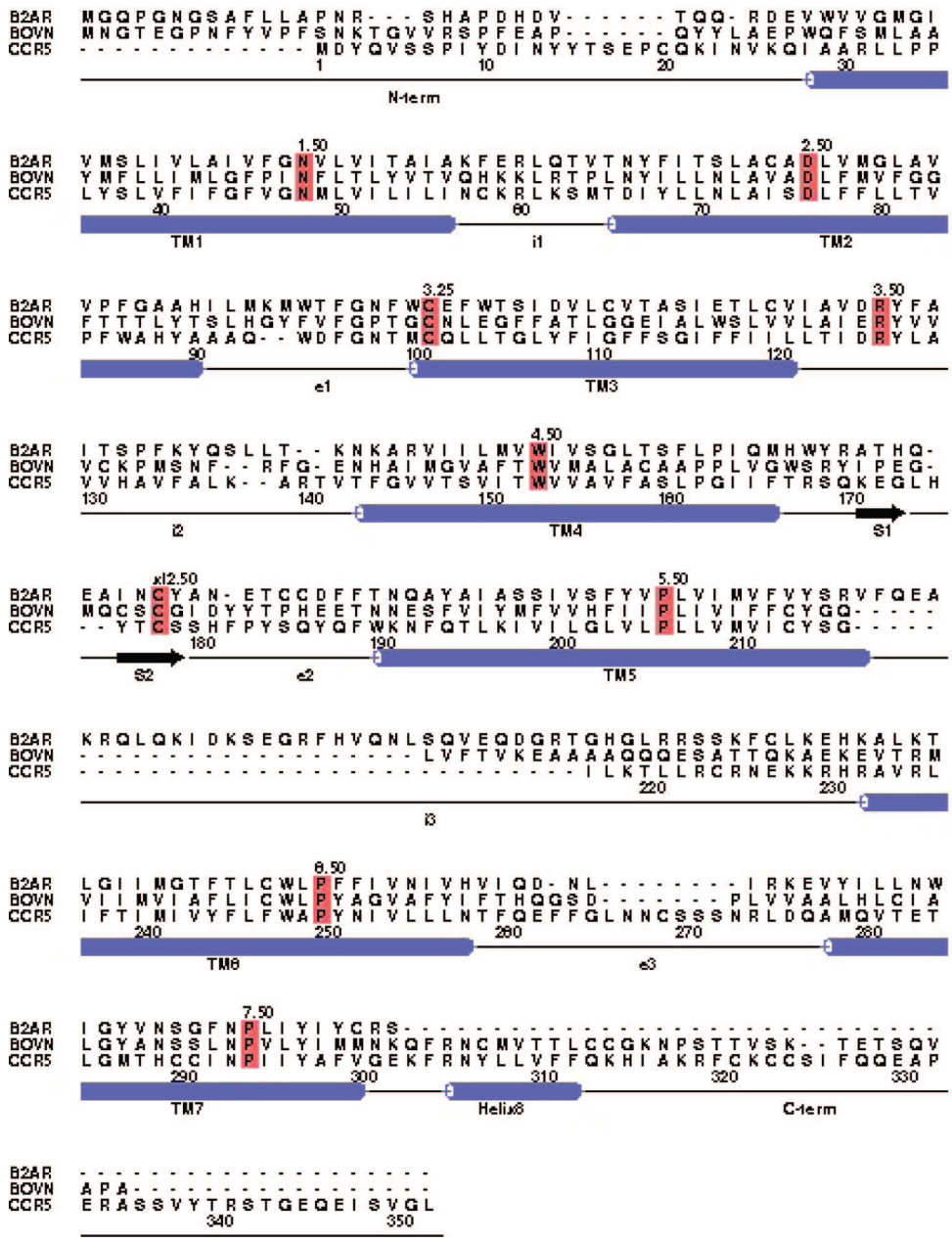

Figure 3. Sequence alignment of human CCR5 (CCR5), bovine rhodopsin (BOVN) (PDB code 1F88), and human β_2AR (B2AR) (PDB code 2RH1). The Ballesteros-Weinstein numbering system was adopted to mark all the conserved amino acid residues among most of the GPCRs and colored in red. The CCR5 protein was numbered accordingly under its sequence. The secondary structure of the CCR5 receptor 3D conformation based on bovine rhodopsin crystal structure was marked out below the sequence.

Table 1. Sequence Homology Analysis of the CCR5 Receptor, Bovine Rhodopsin, and the β_2-Adrenergic Receptor

	CCR5						
homology level %	TM1	TM2	TM3	TM4	TM5	TM6	TM7
bovine rhodopsin (1F88)	53	63	61	57	65	58	43
β_2-adrenergic receptor (2RH1)	50	50	61	52	65	58	57

The coordinates for residues in these regions were obtained by searching for these sequences in the PDB. The adopted conformations of these nonconserved regions all have close similarity to the backbone orientation of the corresponding regions in rhodopsin or β_2AR.

The side chain conformational energies for the entire protein were minimized, while the backbone was constrained followed by a vigorous dynamics simulation to reach an energetically reasonable conformation. Then the local geometry of energy-minimized structure was checked using the InsightII/Homology program. All amino acid residues have reasonable bond lengths and bond angles. The analysis of φ, Ψ, χ_1, and χ_2 angles of the resulting protein conformations was further conducted with Procheck 4.1,[45] and the results were shown in Figure 4 and Table 2. While the model generated based on the β_2AR template has better parameters that that using bovine rhodopsin template, it mainly is because of the parameter difference from the two templates, rather than the modeling operation (see the Supporting Information).

The most significant difference between the crystal structures of bovine rhodopsin and β_2AR is the short α-helical structure of β_2AR in the EL2 loop compared to

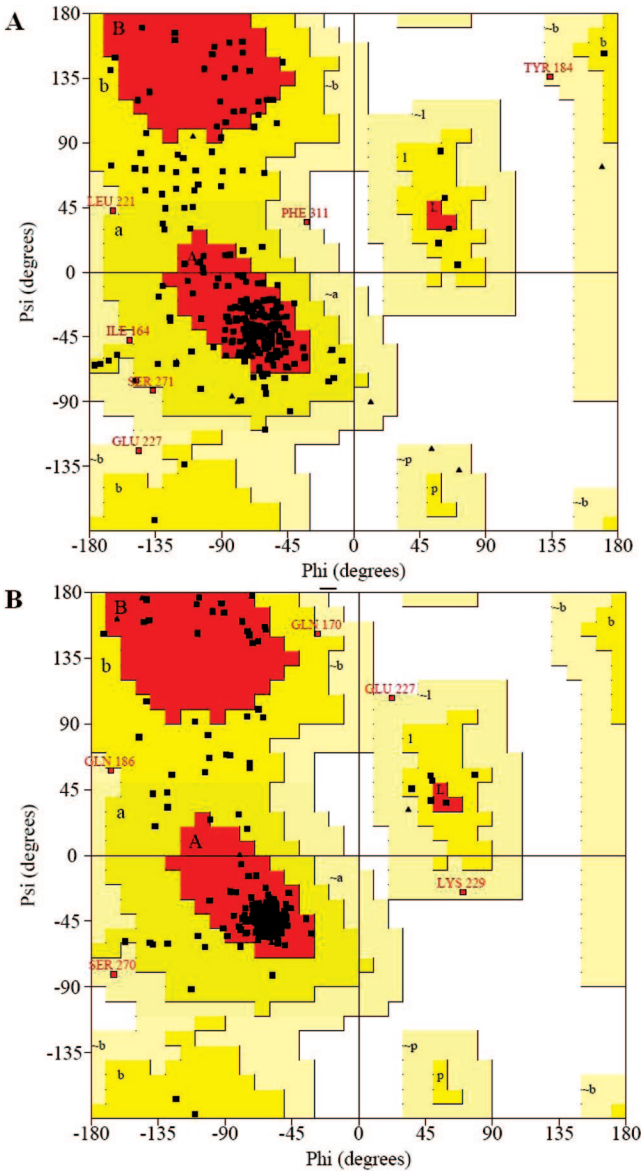

Figure 4. Ramachandran plots of A) rhodopsin-based and B) β_2AR-based CCR5 receptor homology models.

Table 2. Data from the Ramachandran Plot of the Rhodopsin- and β_2-Adrenergic Receptor-Based CCR5 Homology Models

	MFR[a]		AAR[b]		GAR[c]			number of	
model	n	%	n	%	n	%	subtotal[d]	Gly and Pro	total[e]
Rho-based	184	69.7	74	28.0	6	2.3	264	24	288
β_2AR-based	221	83.7	38	14.4	5	1.9	264	24	288

[a] The most favored regions (A, B, and L). [b] The additional allowed regions (a, b, l, and p). [c] The generously allowed regions (-a, -b, -l, and -p). [d] The total number of residues evaluated except glycines and prolines. [e] The total number of amino acids in the receptor models.

the β-sheet structure in bovine rhodopsin. For most GPCRs, the EL2 loop part is very important for ligand recognition with their receptor.[46−54] Thus, we were concerned if an α-helix structure in the EL2 of CCR5 receptor is a reasonable conformation. This possibility (forming an α-helix in the EL2 loop of the CCR5 receptor) was checked with nnpredict (available online from the Cohen group at Department of Cellular and Molecular Pharmacology, University of California, San Francisco) by predicting the secondary structure

```
Sequence ß2AR_E2  M H W Y R A T H Q E A I N C Y A N E T C C D F F T
Prediction        - - - E E - - H H H H H H H - - - - - - - - - - -

Sequence CCR5_E2  F T R S Q K E G L H Y T C S S H F P Y S Q Y Q F W
Prediction        - - - - - H H - - E E E E - - - - - - - - - - - -
```

Figure 5. β_2AR and CCR5 EL2 secondary structure prediction (H = helix, E = strand, - = no prediction).

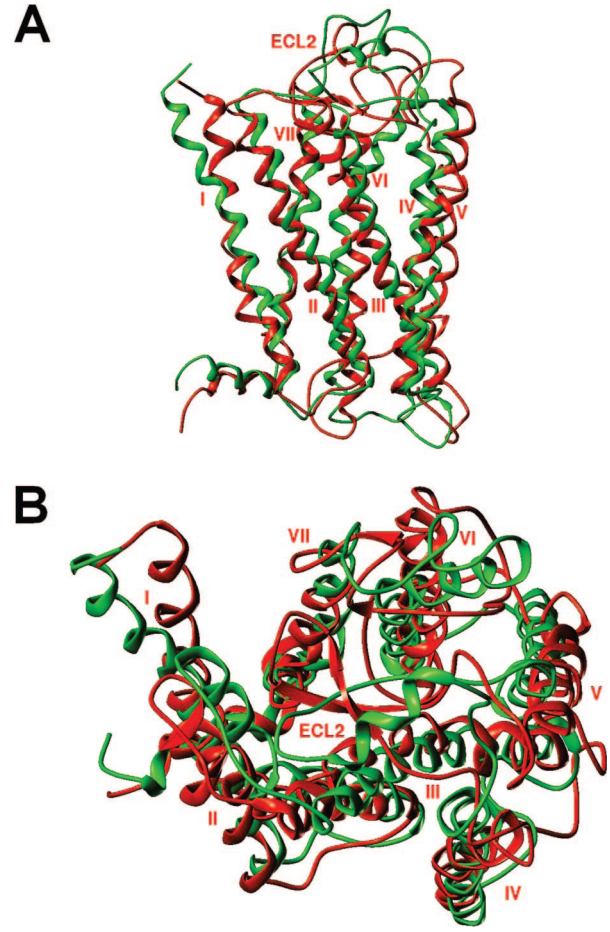

Figure 6. Homology models of CCR5 overlapped in ribbon. The model based on bovine rhodopsin crystal structure is in red, while the one based on β_2AR is in green.

of the EL2 loop. Comparing the nnpredict results for the β_2AR EL2 loop with that of the CCR5 EL2 loop suggests a much lower probability of forming an α-helix structure in CCR5 (Figure 5). Therefore, this domain in the homology model of CCR5 constructed from the β_2AR template may need to be further scrutinized, e.g., by site-directed mutagenesis data.

The differences between the two models were assessed (Figure 6). The overall weighted Root Mean Square Distance (rmsd) value between them was 5.79 Å. In contrast to the rhodopsin-derived model, the TM1 domain of the β_2AR-derived model has a more straight extension. The TM2 to TM7 domains of the two models basically adopted fairly similar orientations. As expected from the discussion above, the EL2 domains were significantly different; i.e., the rhodopsin-derived model presented a β-sheet, while the β_2AR-derived model presented an α-helix conformation. In addition to these differences that largely resulted from their parent templates, different orientations of amino acid residues in these two models transmembrane regions were also observed. These differences may result in each specific binding pocket having different spatial distributions of

Table 3. Top GoldScores for Anibamine and Three Other Known Antagonists Docked in Both Homology Models of CCR5

fitness	anibamine	Aplaviroc	Maraviroc	Vicriviroc
model based on bovine rhodopsin (1F88)	51.57	66.71	54.01	48.83
model based on β_2-adrenergic receptor (2RH1)	50.53	47.64	49.22	43.61

hydrophilic and hydrophobic regions. This will be discussed with the docking study results below.

Binding Site Study of Anibamine As an Antagonist to CCR5. The lowest energy conformation of anibamine and the other antagonists (Aplaviroc, Vicriviroc, and Maraviroc) from the conformation study were first docked interactively into the antagonist binding locus of CCR5 at the upper part of the transmembrane region of the receptor followed by minimization and dynamics simulation of the resulting CCR5-ligand complex. This operation was a necessity because the preliminary automated docking studies revealed no reasonable binding loci in either model due to the stringently steric arrangement of the amino acid residues in the potential binding pocket. By conducting the interactive docking, the ligand binding locus in the receptor was thus identified for the following automated docking study. The orientation of the molecule skeleton in the binding locus was directed by the following: first, the putative ionic interaction between the tertiary nitrogenic group in the ligand and the carboxylic group of Glu283 on TM helix 7 in the receptor; and second, facing the hydrophobic side chain portion of the ligand toward the hydrophobic TM helices. The dockings were validated with a short minimization (500 iterations) and dynamics simulation (1000 steps, 1000 fs total) followed by a more rigorous optimization (minimization of 5000 iterations and a dynamics simulation of 100,000 steps, 100 ps total). In both processes, the backbone of the receptor was fixed to prevent the disruption of the receptor α-helical bundle. The lowest energy conformation from the latter simulation was extracted and saved for analysis.

The automated docking study was conducted by using GOLD 3.1[55] (Genetic Optimization for Ligand Docking) with most default parameters. GOLD permits full ligand flexibility and partial protein flexibility (side chain and backbone flexibility for up to ten user-defined residues). The protein model used for docking each ligand was the lowest energy conformation resulting from the interactive docking studies. The oxygen atom OE1 in Glu283 defined a 10 Å active site radius in the CCR5 receptor. A number of trials were conducted, and the GOLDScores from each docking trial were recorded. The top ten solutions from the final trial were saved. The ligand−receptor complex from the docking result with the highest GOLDScore was extracted (Table 3). It seemed that there was no difference in the binding of anibamine in both models from the viewpoint of GOLD-Scores, while all other three ligands tended to bind better with relatively higher GOLDScores in the homology model of CCR5 based on bovine rhodopsin than the one based on β_2AR.

The final conformations (from the GOLD docking) of the receptor−ligand complexes are illustrated in Figure 7, and the major amino acid residues in the binding sites of the eight complexes are summarized in Table 4. Analyses of the binding pockets of anibamine and the other antagonists revealed that all the antagonists bound to similar hydrophobic pockets in the CCR5 models, while they may occupy different subloci leading to the differences in GOLDScores. For all four ligands studies, the binding pockets in both models were built mainly by TM2, TM3, TM5, TM6, and TM7. Note that residue Glu283 on TM7 is shared by all four antagonists in both models, which is in concordance with the existence and importance of a potentially positively charged core in the ligands.

As an amphiphilic molecule, anibamine carries a positive charge and two highly hydrophobic side chains. Thus, it is not surprising that its binding pocket is composed mainly of aliphatic hydrophobic amino acid residues in both models, while the positively charged nitrogen atom is in the vicinity of Glu283 to form a putative salt bridge. The GOLDScores for each model are not significantly different (Table 3). It should be noted that we do not observe significant interactions between anibamine and the extracellular loop II (EL2) of the protein although Ser179 and Ser180 from EL2 were in the vicinity of the binding locus of anibamine in both homology models of CCR5. Since this loop is believed to be involved in the binding of gp120 to the receptor,[46−51] this observation may explain why anibamine's inhibition affinity to CCR5 was not particularly outstanding. While in the rhodopsin-derived model (Figure 7A,C,E,G) Tyr108 seemed to play important roles in the binding of all four ligands, for anibamine it probably only contributed to the hydrophobic interactions between the ligand and the receptor. Residue Tyr251 seemed to be important to the binding of both anibamine and Aplaviroc. Some amino acid residues were unique for only anibamine; e.g., His289 not only interacted with one of the long aliphatic chains in the ligand molecule but also might confer cation-pi and/or pi-pi stacking interaction with the positively charged core ring system (as His289 was observed in the vicinity). In the β_2AR-derived model (Figure 7B), the two long aliphatic side chains of anibamine adopted a completely different orientation than they do in the rhodopsin-derived model, which lead to a different set of amino acid residues in the binding pocket. Thus, instead of Phe112, Phe109 and Ile164 were part of the hydrophobic pocket. Also, Trp190 and Met279 appeared to play some role in the recognition of anibamine by the CCR5 antagonist binding loci, while His289 was not observed in the binding pocket. Apparently the significant difference from the orientation of the two aliphatic side chains in the molecule provided useful information for future validation of the binding modes as well as for the anibamine derivative design.

In agreement with a very comprehensive site-directed mutagenesis study,[22e] Aplaviroc showed very strong interactions with ECL2 in the rhodopsin-derived model (Figure 7C). For example, Ser180 on EL2 may form hydrogen bond interaction with the molecule. In agreement with the same report, residues Tyr108, Phe112, Tyr251, and Glu283 were all observed in the binding pocket of Aplaviroc, while Asn252 seemed to contribute uniquely to the binding of the molecule. Besides, an ionic or hydrogen bonding interaction between the carboxylic acid moiety of the molecule and Lys197 was also observed in this model. On the other hand, we did not observe a similar interaction between this acidic

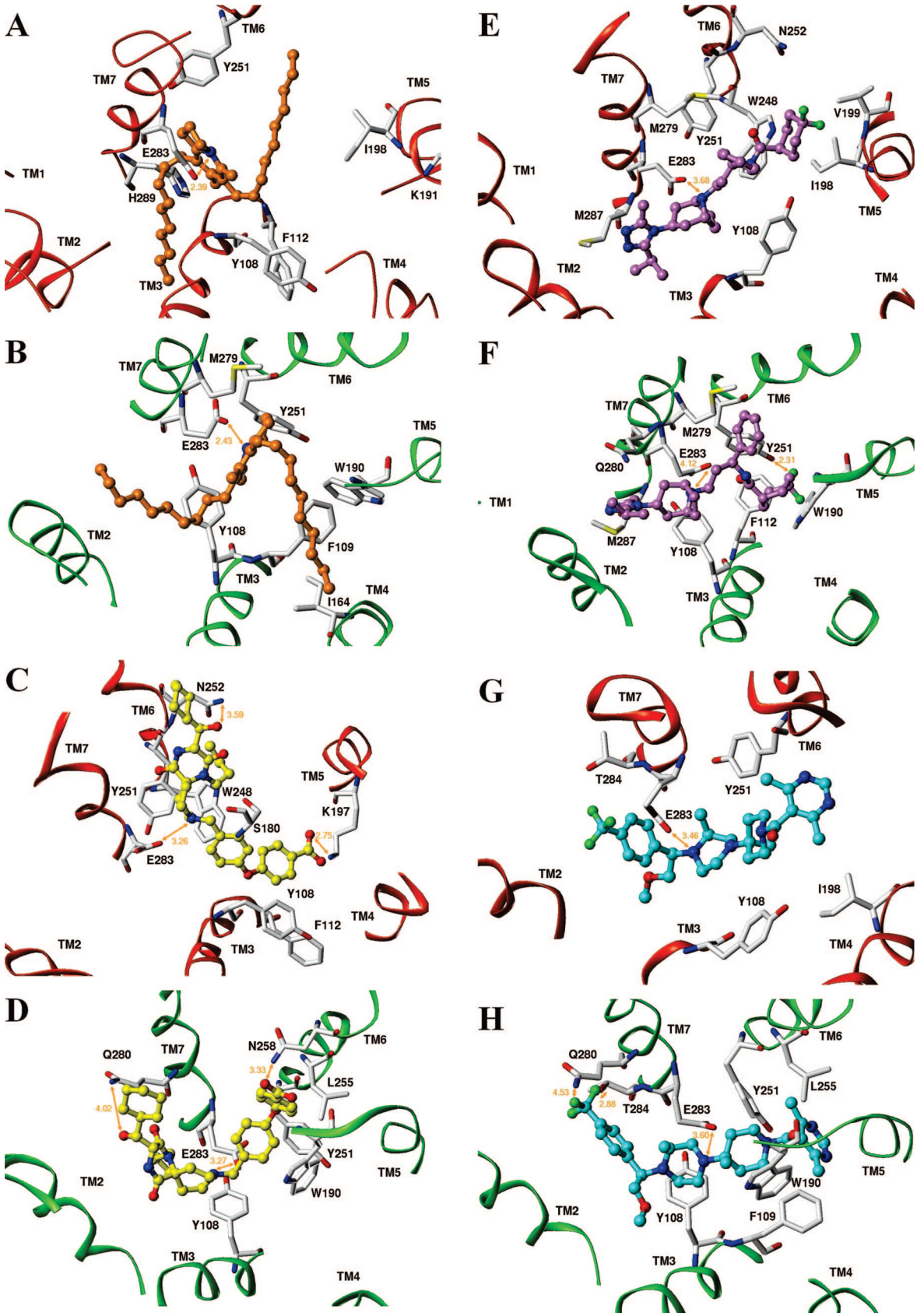

Figure 7. Binding modes of the CCR5 antagonists in the homology model of CCR5 constructed based on bovine rhodopsin (red) and human β_2AR (green). The amino acid residues of the binding pockets were as shown in capped sticks and the ligands were in ball and stick, while the receptor models were in ribbon. ELs and part of TMs were omitted for clarity. Oxygen atoms were in red, fluorine in green, and nitrogen in deep blue. Carbon atoms and the bonds were colored according to the ligands. A and B, anibamine (orange); C and D, Aplaviroc (yellow); E and F, Maraviroc (purple); and G and H, Vicriviroc (cyan).

moiety and Lys191 that was proposed in the literature, while Lys197 seemed to be less important in the same report.[22e]

In the β_2AR-derived CCR5 model (Figure 7D), the binding pocket for Aplaviroc was formed by a totally different set

Table 4. Major Amino Acid Residues in the Binding Pockets of CCR5 Antagonists in the Two Homology Models of the Receptor[a]

	model based on bovine rhodopsin (1F88)	model based on β_2-adrenergic receptor (2RH1)
anibamine	E283, Y251, H289, I198, Y108, F112	E283, Y251, M279, W190, Y108, F109, I164
Aplaviroc	**E283**, ***Y251***, **S180**, **K197**, ***Y108***, **F112,** W248, N252	**E283**, ***Y251***, ***Y108***, Q280, N258, L255, *W190*
Maraviroc	**E283**, **Y251**, **I198**, **Y108**, M279, N252, V199, W248, *M287*	**E283**, **Y251**, **Y108**, M279, Q280, W190, F112, *M287*
Vicriviroc	**E283**, **Y251**, **Y108**, **I198,** T284	**E283**, **Y251**, **Y108,** L255, T284, Q280, W190, *F109*

[a] The residues in **Bold** are consistent with the site-directed mutagenesis report. The residues in *Italics* are in contrary to the site-directed mutagenesis report. The residues in ***Bold/Italics*** are the ones that were reported controversially in the site-directed mutagenesis reports.

of amino acid residues, including Gln280, Asn258, Leu255, Trp190, Tyr251, and Tyr108, with Glu283 as the only exception. Among these residues, Gln280, Asn258, and Leu255 have not been tested in any site-directed mutagenesis studies, while Trp190, Tyr251, and Tyr108 were deemed not essential for ligand binding to CCR5 in another report.[22f] Besides, Ser180 was not observed in the binding locus since EL2 was not involved in the binding pocket formation in this model. This may explain the lower GOLDScore of Aplaviroc in the β_2AR-derived CCR5 model, while plausible hydrogen bonding between Ser180 and the Aplaviroc molecule may contribute significantly in the rhodopsin-derived model.

Maraviroc showed weak interactions with the EL2 region in the rhodopsin-derived model (Figure 7E). Similar to Vicriviroc, Glu283, Tyr108, and Ile198 were important in the binding pocket of Maraviroc in this model, and this was also supported by site-directed mutagenesis studies.[22f] Also, Tyr251 was part of the binding locus in this model, again as supported by site-directed mutagenesis.[22f] Moreover, Trp248 was in the vicinity of the ligand molecule in this model, while it was not supported by the same literature. In the β_2AR-derived CCR5 model (Figure 7F), the binding pocket for Maraviroc showed some similarity to the model based on rhodopsin, e.g. the presence of Tyr251 and Tyr108 in the binding locus. In addition, the involvement of Phe112 and Trp190 has not been tested, while the involvement of Met287 in the binding locus was not supported by site-directed mutagenesis.[22f] While the Goldscores in the two models did not show significant difference, the top score (54.01) for the rhodospin based model was slightly higher than that for the β_2AR based model. This might come from the weak interaction with the EL2 region in the rhodospin based model, which was not observed in the β_2AR based one.

As in anibamine, our rhodopsin-derived model did not indicate strong interactions between Vicriviroc and the EL2 of CCR5, while Glu283, Tyr108, and Ile198 played important roles in the binding pocket (Figure 7G) in agreement with recent site-directed mutagenesis results.[22f] In addition, Tyr251, described as an important residue in the binding pocket of Vicriviroc in the same report, also had significant interactions with the ligand in our model. Hydrophobic interactions of Thr284 with the ligand may be significant based on our observations although this has not been examined experimentally. In the β_2AR-derived CCR5 model (Figure 7H), the binding pocket for Vicriviroc shared some features with the rhodopsin-derived model with some differences arising from variations in orientation of the amino acid residues and the ligand. Again, the model indicates involvement of Tyr251 and Tyr108 with binding, as verified by site-directed mutagenesis.[22f] However, our observation of Phe109 in the binding pocket was contrary to the mutagenesis data. Similarly, the roles of Gln280, Trp190, Thr284, and Leu255 have not, as of yet, been verified. While the major component in the Goldscores was the van der Waals interactions between the ligand and the receptor, no apparent difference was observed for either model.

CONCLUSION

Two homology models of chemokine receptor CCR5 were constructed based on the crystal structures of bovine rhodopsin and the human β_2-adrenergic receptor, respectively. Anibamine, the first natural product CCR5 antagonist, along with other three well-known CCR5 antagonists were docked into these two models. The binding pockets for these ligands were characterized and compared with the reported site-directed mutagenesis studies. Our modeling studies indicate that the binding pockets for all four CCR5 antagonists are located in the transmembrane (TM) part of the protein near Glu283. This position allows a putative ionic interaction with the quaternary nitrogen that is a common feature of the CCR5 antagonists. While some ligands showed a very strong interaction with extracellular loop 2 in the rhodopsin template-based model, others did not, which may directly influence their GOLDScores (binding fitness). In both the rhodopsin-derived model and the β_2AR-derived model, all four ligands tended to adopt a similar binding locus, while for each ligand, the binding modes and orientations were somewhat different between these two models. This is certainly related to the different 3D conformations of the TM domains and orientations of the amino acid side chains in the crystal structure template the models were based on. Most importantly for our future work is that anibamine shares many common binding features with the other known CCR5 ligands in each model, thus suggesting that its inhibition activity may stem from binding to the CCR5 antagonist binding locus.

While from our studies, both the crystal structures of bovine rhodopsin and human β_2AR seemed to be reasonable templates to conduct homology modeling operation for CCR5 receptor, the rhodopsin-derived model received more support from the reported site-directed mutagenesis studies for the known CCR5 antagonists, while the binding pockets for those ligands identified from the β_2AR-derived model need to be further verified by more extensive experimental studies.

Anibamine is an interesting lead compound for anti-HIV drug discovery. It is the first and only natural product CCR5 antagonist identified such far, and because of its unique skeleton, the recently reported flexible total synthesis of anibamine opens up a number of research directions. In particular, the pursuing of the next generation molecular design based on the unique binding features of anibamine may yield a clinically relevant CCR5 antagonist. The binding

mode study of anibamine in CCR5 homology models reported herein will be beneficial to the future study in novel drug design and development.

COMPUTATIONAL METHODS

The sequence of human chemokine receptor CCR5 was obtained from http://www.expasy.org (Swiss-Prot and TrEMBL), and the crystal structures of bovine rhodopsin and human β_2AR were downloaded from http://www.rcsb.org. All computations were performed on SGI Octane2 workstations (Silicon Graphics, Inc., Mountain View, CA).

Homology modeling was carried out using the Homology and Discover modules of the InsightII package (Accelrys, San Diego, CA). The sequence alignment was conducted automatically by applying different scoring matrices, gap penalty, and gap length penalty parameters in order to achieve the highest sequence homology. Then the coordinates for the amino acid residues in the structurally conserved regions of CCR5 were assigned following the corresponding residues in the CCR5 receptor. The coordinates for the amino acid residues of the CCR5 receptor in the structurally nonconserved regions were obtained by searching the protein database with the InsightII/Homology/Loop_Search module. After the completion of the amino acid residue coordinates assignment, the conformation of the whole protein was minimized with the backbone constrained. A brief minimization (2,000 iterations) and dynamics simulation (10,000 step, 1 fs each step) was conducted to relax major steric clashes introduced during the coordinate assignment. Further vigorous simulation (minimization 10,000 iterations and dynamics 100,000 steps, 100 ps total) was conducted to produce an energetically reasonable conformation. The CFF91 force field was applied, while the minimization was terminated until the maximum derivative is less than 0.001 kcal/mol.

All the small (ligand) molecules were built using InsightII/Builder Module. Minimizations with steepest descent followed by conjugate gradient were performed to generate the lowest energy conformation for each ligand studied (CFF91 force field and default termination values were adopted). Then a molecular dynamics simulation was performed (an equilibration phase of 1000 fs at 300 K, followed by a collection phase of 5000 fs at the same temperature) to further study the small molecule conformation. We used the lowest energy conformation of the small molecules in water extracted from the 5 ps molecular dynamics calculations, as the initial configuration for docking into the proposed binding site of the CCR5 receptor. The ligand was modeled in its nitrogen-protonated form when applicable.

The interactive docking study was conducted in the Discover module of InsightII. The ligands were docked in the upper portion of transmembrane region of the receptor, following orientations reported in the literature.[22] Each ligand−receptor complex was minimized in the gas phase first with the backbone of the receptor fixed, but all the side chain atoms were left unconstrained. The optimized conformation was then used as the initial configuration for molecular dynamics simulations. For each complex, a short-term steepest descent energy minimization (500 iterations) and a dynamics simulation (1000 step, 1 fs each step) was conducted to validate the initial docking conformation. This was followed by another simulation minimization (5000 iterations), and 100,000 steps of dynamics were conducted with an initial 2000 steps equilibration. The total simulation time was 102 ps. Again the CFF91 force field and default termination value (0.01 kcal/mol) was adopted.

Automated docking was conducted with GOLD.[55] Default parameters were adopted except that the docking locus was defined as 10 Å around the OE1 of Glu283 on helix 7 of CCR5. Based on the fitness scores and binding orientation of the ligands, the best solution of GOLD binding (among top ten solutions that were recorded) was selected and merged into the structure of CCR5 receptor. The combined structures of the ligand and CCR5 receptor were minimized together in order to allowing the receptor to adopt the presence of ligand. After that, the ligand was removed from the complex, and the resulting structure was evaluated by PROCHECK again. The docking results were summarized in Table 3. Finally, all the models were optimized by molecular dynamics simulation, using SYBYL7.3 with default parameters except for the following: length - 100,000 fs, snapshot every 25 fs; time step - 1 fs, dielectric constant 4.0.

The PDB files of the homology models are available from the corresponding author upon request.

ACKNOWLEDGMENT

This work was supported partially by U.S. Army Prostate Cancer Research Program PC073739 and NIH/NIAID AI69975 and AI074461. We would like to thank Philip Mosier for his generous help in Procheck documents.

Supporting Information Available: Goldscore summary: the top ten scores from the last trial in the automatic docking for all four ligands and the Ramachandran plots of bovine rhodopsin and β_2AR crystal structures. This material is available free of charge via the Internet at http://pubs.acs.org.

REFERENCES AND NOTES

(1) 2006. Report on the Global AIDS Epidemic: Executive Summary, A UNAIDS 10th Anniversary Special Edition.
(2) HIV Infection and AIDS: an Overview, NIAID Fact Sheet. http://www.niaid.nih.gov/factsheets/hivinf.htm (accessed Nov 7, 2008).
(3) Littman, D. R. Chemokine Receptors: Keys to AIDS Pathogenesis. *Cell* **1998**, *93*, 677–680.
(4) Chinen, J.; Shearer, W. T. Molecular virology and immunology of HIV infection. *J. Allergy Clin. Immunol.* **2002**, *110*, 189–198.
(5) Kedzierska, K.; Crowe, S. M.; Turville, S.; Cunningham, A. L. The influence of cytokines, chemokines and their receptors on HIV-1 replication in monocytes and macrophages. *Rev. Med. Virol.* **2003**, *13*, 39–56.
(6) Schwarz, M. K.; Wells, T. N. C. New Therapeutics that Modulate Chemokine Networks. *Nat. Rev. Drug Discovery* **2002**, *1*, 347–358.
(7) Howard, O. M.; Oppenheim, J. J.; Wang, J. M. Chemokines as molecular targets for therapeutic intervention. *J. Clin. Immunol.* **1999**, *19*, 280–292.
(8) Samson, M.; Libert, F.; Doranz, B. J.; Rucker, J.; Liesnard, C.; Farber, C. M.; Saragosti, S.; Lapouméroulie, C.; Cognaux, J.; Forceille, C.; Muyldermans, G.; Verhofstede, C.; Burtonboy, G.; Georges, M.; Imai, T.; Rana, S.; Yi, Y.; Smyth, R. J.; Collman, R. J.; Doms, R. W.; Vassart, G.; Parmentier, M. Resistance to HIV-1 infection in Caucasian individuals bearing mutant alleles of the CCR-5 chemokine receptor gene. *Nature* **1996**, *382*, 722–725.
(9) Liu, R.; Paxton, W. A.; Choe, S.; Ceradini, D.; Marti, S. R.; Horuk, R.; MacDonald, M. E.; Stuhlmann, H.; Koup, R. A.; Landau, N. R. Homozygous Defect in HIV-1 Coreceptor Accounts for Resistance of Some Multiply-Exposed Individuals to HIV-1 Infection. *Cell* **1996**, *86*, 367–377.
(10) Fernandez, E. J.; Lolis, E. Structure, function and inhibition of chemokines. *Annu. Rev. Pharmacol. Toxicol.* **2002**, *42*, 469–499.
(11) Strizki, J. M.; Xu, S.; Wagner, N. E.; Wojcik, L.; Liu, J.; Hou, Y.; Endres, M.; Palani, A.; Shapiro, S.; Clader, J. W.; Greenlee, W. J.;

Tagat, J. R.; McCombie, S.; Cox, K.; Fawzi, A. B.; Chou, C. C.; Pugliese-Sivo, C.; Davies, L.; Moreno, M. E.; Ho, D. D.; Trkola, A.; Stoddart, C. A.; Moore, J. P.; Reyes, G. R.; Baroudy, B. M. Sch-C(SCH351125), an orally bioavailable, small molecule antagonist of the chemokine receptor CCR5, is a potent inhibitor of HIV-1 infection *in vitro* and *in vivo*. *Proc. Natl. Acad. Sci. U.S.A.* **2001**, *98*, 12718–12723.

(12) (a) Tagat, J. R.; McCombie, S. W.; Nazareno, D.; Labroli, M. A.; Xiao, Y.; Steensma, R. W.; Strizki, J. M.; Baroudy, B. M.; Cox, K.; Lachowicz, J.; Varty, G.; Watkins, R. Piperazine-Based CCR5 Antagonists as HIV-1 Inhibitors. IV. Discovery of 1-[(4,6-Dimethyl-5-pyrimidinyl)carbonyl]-4-[4-{2-methoxy-1(*R*)-4-(trifluoromethyl)phenyl}ethyl-3(*S*)-methyl-1-piperazinyl]-4-methylpiperidine(Sch-417690/Sch-D), a Potent, Highly Selective, and Orally Bioavailable CCR5 Antagonist. *J. Med. Chem.* **2004**, 2405–2408. (b) Strizki, J. M.; Tremblay, C.; Xu, S.; Wojcik, L.; Wagner, N.; Gonsiorek, W.; Hipkin, R. W.; Chou, C. C.; Pugliese-Sivo, C.; Xiao, Y.; Tagat, J. R.; Cox, K.; Priestley, T.; Sorota, S.; Huang, W.; Hirsch, M.; Reyes, G. R.; Baroudy, B. M. Discovery and characterization of vicriviroc (Sch-417690), a CCR5 antagonist with potent activity against human immunodeficiency virus type 1. *Antimicrob. Agents Chemother.* **2005**, *49*, 4911–9.

(13) (a) Maeda, K.; Nakata, H.; Koh, Y.; Miyakawa, T.; Ogata, H.; Takaoka, Y.; Shibayama, S.; Sagawa, K.; Fukushima, D.; Moravek, J.; Koyanagi, Y.; Mitsuya, H. Spirodiketopiperazine-based CCR5 inhibitor which preserves CC-chemokine/CCR5 interactions and exerts potent activity against R5 human immunodeficiency virus type 1 in vitro. *J. Virol.* **2004**, *78*, 8654. (b) Nichols, W. G.; Steel, H. M.; Bonny, T.; Adkison, K.; Curtis, L.; Millard, J.; Kabeya, K.; Clumeck, N. Hepatotoxicity observed in clinical trials of aplaviroc (873140). *Antimicrob. Agents Chemother.* **2008**, *52*, 858–65.

(14) (a) Dorr, P.; Westby, M.; Dobbs, S.; Griffin, P.; Irvine, B.; Macartney, M.; Mori, J.; Rickett, G.; Smith-Burchnell, C.; Napier, C.; Webster, R.; Armour, D.; Price, D.; Stammen, B.; Wood, A.; Perros, M. Maraviroc (UK-427,857), a potent, orally bioavailable, and selective small-molecule inhibitor of chemokine receptor CCR5 with broad-spectrum anti-human immunodeficiency virus type 1 activity. *Antimicrob. Agents Chemother.* **2005**, *49*, 4721–32. (b) FDA Panel Backs HIV Drug, Pfizer Treatment Blocks Pathway Used to Infect Cells, *Wall Street Journal*, April 25, 2007. (c) FDA Voices Concerns Over New HIV Drug Class. *Wall Street Journal*, April 21, 2007. (d) AIDSinfo-A Service of the U.S. Department of Health and Human Services. http://aidsinfo.nih.gov/DrugsNew/DrugDetailNT.aspx?MenuItem=Drugs&Search=On&int_id=408 (accessed Nov 7, 2008).

(15) (a) Verdine, G. L. The Combinatorial Chemistry of Nature. *Nature* **1996**, *384*, 1–3. (b) Feher, M.; Schmidit, J. M. Property distributions: differences between drugs, natural products, and molecules from combinatorial chemistry. *J. Chem. Inf. Comput. Sci.* **2003**, *43*, 218–27.

(16) Jayasuriya, H.; Herath, K. B.; Ondeyka, J. G.; Polishook, J. D.; Bills, G. F.; Dombrowski, A. W.; Springer, M. S.; Siciliano, S.; Malkowitz, L.; Sanchez, M.; Guan, Z.; Tiwari, S.; Stevenson, D. W.; Borris, R. P.; Singh, S. B. Isolation and structure of antagonists of chemokine receptor (CCR5). *J. Nat. Prod.* **2004**, *67*, 1036–38.

(17) Li, G.; Watson, K.; Buckheit, R. W.; Zhang, Y. Total Synthesis of Anibamine, a Novel Natural Product as a Chemokine Receptor CCR5 Antagonist. *Org. Lett.* **2007**, *9*, 2043–2046.

(18) (a) Lynch, C. L.; Willoughby, C. A.; Hale, J. J.; Holson, E. J.; Budhu, R. J.; Gentry, A. L.; Rosauer, K. G.; Caldwell, C. G.; Chen, P.; Mills, S. G.; MacCoss, M.; Berk, S.; Chen, L.; Chapman, K. T.; Malkowitz, L.; Springer, M. S.; Siciliano, S. J.; Cascieri, M. A.; Carella, A.; Carver, G.; Holmes, K.; Schleif, W. A.; Danzeisen, R.; Hazuda, D.; Kessler, J.; Lineberger, J.; Miller, M.; Emini, E. A. 1,3,4-Trisubstituted pyrrolidine CCR5 receptor antagonists: modifications of the arylpropylpiperidine side chains. *Bioorg. Med. Chem. Lett.* **2003**, *13*, 119–23. (b) Shen, D. M.; Shu, M.; Mills, S. G.; Chapman, K. T.; Malkowitz, L.; Springer, M. S.; Gould, S. L.; DeMartino, J. A.; Siciliano, S. J.; Kwei, G. Y.; Carella, A.; Carver, G.; Holmes, K.; Schleif, W. A.; Danzeisen, R.; Hazuda, D.; Kessler, J.; Lineberger, J.; Miller, M. D.; Emini, E. A. Antagonists of human CCR5 receptor containing 4-(pyrazolyl)piperidine side chains. Part 1: Discovery and SAR study of 4-pyrazolylpiperidine side chains. *Bioorg. Med. Chem. Lett.* **2004**, *14*, 935–9. (c) Shen, D. M.; Shu, M.; Willoughby, C. A.; Shah, S.; Lynch, J. J.; Hale, S. G.; Mills, K. T.; Chapman, L.; Malkowitz, M. S.; Springer, S. L.; Gould, C. L.; DeMartino, J. A.; Siciliano, S. J.; Lyons, K.; Pivnichny, J. V.; Kwei, G. Y.; Carella, A.; Carver, G.; Holmes, K.; Schleif, W. A.; Danzeisen, R.; Hazuda, D.; Kessler, J.; Lineberger, J.; Miller, M. D.; Emini, E. A. Antagonists of human CCR5 receptor containing 4-(pyrazolyl)piperidine side chains. Part 2: Discovery of potent, selective, and orally bioavailable compounds. *Bioorg. Med. Chem. Lett.* **2004**, *14*, 941–5. (d) Shu, M.; Loebach, J. L.; Parker, K. A.; Mills, S. G.; Chapman, K. T.; Shen, D. M.; Malkowitz, L.; Springer, M. S.; Gould, S. L.; DeMartino, J. A.; Siciliano, S. L.; Salvo, J. D.; Lyons, K.; Pivnichny, J. V.; Kwei, G. Y.; Carella, A.; Carver, G.; Holmes, K.; Schleif, W. A.; Danzeisen, R.; Hazuda, D.; Kessler, J.; Lineberger, J.; Miller, M. D.; Emini, E. A. Antagonists of human CCR5 receptor containing 4-(pyrazolyl)piperidine side chains. Part 3: SAR studies on the benzylpyrazole segment. *Bioorg. Med. Chem. Lett.* **2004**, *14*, 947–952.

(19) Dorn, C. P.; Finke, P. E.; Oates, B.; Budhu, R. J.; Mills, S. G.; MacCoss, M.; Malkowitz, L.; Springer, M. S.; Daugherty, B. L.; Gould, S. L.; DeMartino, J. A.; Siciliano, S. J.; A.; Carella, A.; Carver, G.; Holmes, K.; Danzeisen, R.; Hazuda, D.; Kessler, J.; Lineberger, J.; Miller, M. D.; Emini, E. A. Antagonists of the human CCR5 receptor as anti-HIV-1 agents. part 1: discovery and initial structure-activity relationships for 1 -amino-2-phenyl-4-(piperidin-1-yl)butanes. *Bioorg. Med. Chem. Lett.* **2001**, *11*, 259–264.

(20) Palani, A.; Shapiro, S.; Clader, J. W.; Greenlee, W. J.; Cox, K.; Strizki, J.; Endres, M.; Baroudy, B. M. Discovery of 4-[(Z)-(4-bromophenyl)-(ethoxyimino)methyl]-1′-[(2,4-dimethyl-3-pyridinyl)carbonyl]-4′-methyl-1,4′-bipiperidine N-oxide (SCH 351125): an orally bioavailable human CCR5 antagonist for the treatment of HIV infection. *J. Med. Chem.* **2001**, *44*, 3339–42.

(21) Shiraishi, M.; Aramaki, Y.; Seto, M.; Imoto, H.; Nishikawa, Y.; Kanzaki, N.; Okamoto, M.; Sawada, H.; Nishimura, O.; Baba, M.; Fujino, M. Discovery of novel, potent, and selective small-molecule CCR5 antagonists as anti-HIV-1 agents: synthesis and biological evaluation of anilide derivatives with a quaternary ammonium moiety. *J. Med. Chem.* **2000**, *43*, 2049–63.

(22) (a) Dragic, T.; Trkola, A.; Thompson, D. A. D.; Cormier, E. G.; Kajumo, F. A.; Maxwel, E.; Lin, S. W.; Ying, W.; Smith, S. O.; Sakmar, T. P.; Moore, J. P. A Binding Pocket for a Small Molecule Inhibitor of HIV-1 Entry Within the Transmembrane Helices of CCR5. *Proc. Natl. Acad. Sci. U.S.A.* **2000**, *97*, 5639–5644. (b) Paterlini, M. G. Structure Modeling of the Chemokine Receptor CCR5: Implication for Ligand Binding and Selectivity. *Biophys. J.* **2002**, *83*, 3012–31. (c) Castonguay, L. A.; Weng, Y.; Adolfsen, W.; Salvo, J. D.; Kilburn, R.; Caldwell, C. G.; Daugherty, B. L.; Finke, P. E.; Hale, J. J.; Lynch, C. L.; Mills, S. G.; MacCoss, M.; Springer, M. S.; DeMartino, J. A. Binding of 2-Aryl-4-(piperidin-1-yl)butanamines and 1,3,4-Trisubstituted Pyrrolidines to Human CCR5: A Molecular Modeling-Guided Mutagenesis Study of the Binding Pocket. *Biochemistry* **2003**, *42*, 1544–1550. (d) Song, M.; Breneman, C. M.; Sukumar, N. 3D QSAR Analyses of Piperidine-based CCR5 Receptor Antagonists. *Bioorg. Med. Chem.* **2004**, *12*, 489–499. (e) Maeda, K.; Das, D.; Ogata-Aoki, H.; Nakata, H.; Miyakawa, T.; Tojo, Y.; Norman, R.; Takaoka, Y.; Ding, J.; Arnold, G. F.; Arnold, E.; Mitsuya, H. Structural and molecular interactions of CCR5 inhibitors with CCR5. *J. Biol. Chem.* **2006**, *281*, 12688–98. (f) Kondru, R.; Zhang, J.; Ji, C.; Mirzadegan, T.; Rotstein, D.; Sankuratri, S.; Dioszegi, M. Molecular interactions of CCR5 with major classes of small-molecule anti-HIV CCR5 antagonists. *Mol. Pharmacol.* **2008**, *73* (3),), 789–800.

(23) (a) Müller, G. Towards 3D structures of G protein-coupled receptors: a multidisciplinary approach. *Curr. Med. Chem.* **2000**, *7* (9), 861–88. (b) Klabunde, T.; Hessler, G. Drug design strategies for targeting G-protein-coupled receptors. *Chembiochem.* **2002**, *3* (10), 928–44. (c) Chou, K. C. Structural bioinformatics and its impact to biomedical science. *Curr. Med. Chem.* **2004**, *11*, 2105–2134. (d) Filizola, M.; Weinstein, H. The study of G-protein coupled receptor oligomerization with computational modeling and bioinformatics. *FEBS J.* **2005**, *272* (12), 2926–38. (e) Lundstrom, K. Latest development in drug discovery on G protein-coupled receptors. *Curr. Protein Pept. Sci.* **2006**, *7* (5), 465–70.

(24) (a) Lowrie, J. F.; Delisle, R. K.; Hobbs, D. W.; Diller, D. J. The different strategies for designing GPCR and kinase targeted libraries. *Comb. Chem. High Throughput Screening* **2004**, *7* (5), 495–510. (b) Chou, K. C.; Wei, D. Q.; Zhong, W. Z. Binding mechanism of coronavirus main proteinase with ligands and its implication to drug design against SARS. *Biochem. Biophys. Res. Commun.* **2003**, *308*, 148–151. (c) Ashton, M.; Charlton, M. H.; Schwarz, M. K.; Thomas, R. J.; Whittaker, M. The selection and design of GPCR ligands: from concept to the clinic. *Comb. Chem. High Throughput Screen.* **2004**, *7* (5), 441–52. (d) Zhang, R.; Wei, D. Q.; Du, Q. S.; Chou, K. C. Molecular modeling studies of peptide drug candidates against SARS. *Med. Chem.* **2006**, *2*, 309–314. (e) Li, Y.; Wei, D. Q.; Gao, W. N.; Gao, H.; Liu, B. N.; Huang, C. J.; Xu, W. R.; Liu, D. K.; Chen, H. F.; Chou, K. C. Computational approach to drug design for oxazolidinones as antibacterial agents. *Med. Chem.* **2007**, *3*, 576–582. (f) Gao, W. N.; Wei, D. Q.; Li, Y.; Gao, H.; Xu, W. R.; Li, A. X.; Chou, K. C. Agaritine and its derivatives are potential inhibitors against HIV proteases. *Med. Chem.* **2007**, *3*, 221–226. (g) Zheng, H.; Wei, D. Q.; Zhang, R.; Wang, C.; Wei, H.; Chou, K. C. Screening for New Agonists against Alzheimer's Disease. *Med. Chem.* **2007**, *3*, 488–493. (h) Jacobson, K. A.; Gao, Z. G.; Liang, B. T. Neoceptors: reengineering

GPCRs to recognize tailored ligands. *Trends Pharmacol. Sci.* **2007**, *28* (3), 111–6. (i) Wang, J. F.; Wei, D. Q.; Chen, C.; Li, Y.; Chou, K. C. Molecular modeling of two CYP2C19 SNPs and its implications for personalized drug design. *Protein Pept. Lett.* **2008**, *15*, 27–32.

(25) (a) Chou, K. C.; Nemethy, G.; Scheraga, H. A. Energetic approach to packing of a-helices: 2. General treatment of nonequivalent and nonregular helices. *J. Am. Chem. Soc.* **1984**, *106*, 3161–3170. (b) Chou, K. C.; Maggiora, G. M.; Nemethy, G.; Scheraga, H. A. Energetics of the structure of the four-α helix bundle in proteins. *Proc. Natl. Acad. Sci. U.S.A.* **1988**, *85*, 4295–4299. (c) Lomize, A. L.; Pogozheva, I. D.; Mosberg, H. I. Structural organization of G-protein-coupled receptors. *J. Comput.-Aided Mol. Des.* **1999**, *13* (4), 325–53. (d) Picone, R. P.; Fournier, D. J.; Makriyannis, A. Ligand based structural studies of the CB1 cannabinoid receptor. *J. Pept. Res.* **2002**, *60* (6), 348–56.

(26) (a) Sirois, S.; Wei, D. Q.; Du, Q. S.; Chou, K. C. Virtual Screening for SARS-CoV Protease Based on KZ7088 Pharmacophore Points. *J. Chem. Inf. Comput. Sci.* **2004**, *44*, 1111–1122. (b) Schlegel, B.; Laggner, C.; Meier, R.; Langer, T.; Schnell, D.; Seifert, R.; Stark, H.; Höltje, H. D.; Sippl, W. Generation of a homology model of the human histamine H(3) receptor for ligand docking and pharmacophore-based screening. *J. Comput.-Aided Mol. Des.* **2007**, *21* (8), 437–53.

(27) (a) Chou, K. C. Energy-optimized structure of antifreeze protein and its binding mechanism. *J. Mol. Biol.* **1992**, *223*, 509–517. (b) Mehler, E. L.; Periole, X.; Hassan, S. A.; Weinstein, H. Key issues in the computational simulation of GPCR function: representation of loop domains. *J. Comput.-Aided Mol. Des.* **2002**, *16* (11), 841–53. (c) Carlacci, L.; Millard, C. B.; Olson, M. A. Conformational energy landscape of the acyl pocket loop in acetylcholinesterase: a Monte Carlo-generalized Born model study. *Biophys. Chem.* **2004**, *111* (2), 143–57.

(28) (a) Zhou, G. P.; Deng, M. H. An extension of Chou's graphical rules for deriving enzyme kinetic equations to system involving parallel reaction pathways. *Biochem. J.* **1984**, *222*, 169–176. (b) Myers, D.; Palmer, G. Microcomputer tools for steady-state enzyme kinetics. *Bioinformatics* **1985**, *1*, 105–110. (c) Dussert, C.; Rasigni, M.; Palmari, J.; Rasigni, G.; Llebaria, A.; Marty, F. Minimal spanning tree analysis of biological structures. *J. Theor. Biol.* **1987**, *125* (3), 317–23. (d) Chou, K. C. Graphical rules in steady and non-steady enzyme kinetics. *J. Biol. Chem.* **1989**, *264*, 12074–12079. (e) Chou, K. C. Applications of graph theory to enzyme kinetics and protein folding kinetics. Steady and non-steady state systems. *Biophys. Chem.* **1990**, *35*, 1–24. (f) Wernisch, L.; Hunting, M.; Wodak, S. J. Identification of structural domains in proteins by a graph heuristic. *Proteins* **1999**, *35* (3), 338–52. (g) Andraos, J. Kinetic plasticity and the determination of product ratios for kinetic schemes leading to multiple products without rate laws: new methods based on directed graphs. *Can. J. Chem.* **2008**, *86*, 342–357.

(29) (a) Chou, K. C.; Zhou, G. P. Role of the protein outside active site on the diffusion-controlled reaction of enzyme. *J. Am. Chem. Soc.* **1982**, *104*, 1409–1413. (b) Klenin, K. V.; Langowski, J. Modeling of intramolecular reactions of polymers: an efficient method based on Brownian dynamics simulations. *J. Chem. Phys.* **2004**, *121* (10), 4951–60. (c) Sung, B. J.; Yethiraj, A. Molecular-dynamics simulations for nonclassical kinetics of diffusion-controlled bimolecular reactions. *J. Chem. Phys.* **2005**, *123* (11), 114503–5. (d) Cheng, Y.; Cheng, X.; Radić, Z.; McCammon, J. A. Acetylcholinesterase: mechanisms of covalent inhibition of wild-type and H447I mutant determined by computational analyses. *J. Am. Chem. Soc.* **2007**, *129* (20), 6562–70.

(30) (a) Chou, K. C. Low-frequency collective motion in biomacromolecules and its biological functions. *Biophys. Chem.* **1988**, *30*, 3–48. (b) Chou, K. C. Low-frequency resonance and cooperativity of hemoglobin. *Trends Biochem. Sci.* **1989**, *14*, 212.

(31) (a) Du, Q. S.; Mezey, P. G.; Chou, K. C. Heuristic Molecular Lipophilicity Potential (HMLP): A 2D-QSAR Study to LADH of Molecular Family Pyrazole and Derivatives. *J. Comput. Chem.* **2005**, *26*, 461–470. (b) Evers, A.; Hessler, G.; Matter, H.; Klabunde, T. Virtual screening of biogenic amine-binding G-protein coupled receptors: comparative evaluation of protein- and ligand-based virtual screening protocols. *J. Med. Chem.* **2005**, *48* (17), 5448–65. (c) Rolland, C.; Gozalbes, R.; Nicolaï, E.; Paugam, M. F.; Coussy, L.; Barbosa, F.; Horvath, D.; Revah, F. G-protein-coupled receptor affinity prediction based on the use of a profiling dataset: QSAR design, synthesis, and experimental validation. *J. Med. Chem.* **2005**, *48* (21), 6563–74. (d) Gonzalez-Diaz, H.; Sanchez-Gonzalez, A.; Gonzalez-Diaz, Y. 3D-QSAR study for DNA cleavage proteins with a potential anti-tumor ATCUN-like motif. *J. Inorg. Biochem.* **2006**, *100*, 1290–1297. (e) Sewing, A.; Cawkill, D. High-throughput lead finding and optimisation for GPCR targets. *Ernst Schering Found Symp. Proc.* **2006**, *2*, 249–67. (f) Tropsha, A.; Wang, S. X. QSAR modeling of GPCR ligands: methodologies and examples of applications. *Ernst Schering Found Symp. Proc.* **2006**, *2*, 49–73. (g) Costanzi, S.; Tikhonova, I. G.; Ohno, M.; Roh, E. J.; Joshi, B. V.; Colson, A. O.; Houston, D.; Maddileti, S.; Harden, T. K.; Jacobson, K. A. P2Y1 antagonists: combining receptor-based modeling and QSAR for a quantitative prediction of the biological activity based on consensus scoring. *J. Med. Chem.* **2007**, *50* (14), 3229–41. (h) Du, Q. S.; Huang, R. B.; Wei, Y. T.; Du, L. Q.; Chou, K. C. Multiple Field Three Dimensional Quantitative Structure-Activity Relationship (MF-3D-QSAR). *J. Comput. Chem.* **2008**, *29*, 211–219. (i) Prado-Prado, F. J.; Gonzalez-Diaz, H.; de la Vega, O. M.; Ubeira, F. M.; Chou, K. C. Unified QSAR approach to antimicrobials. Part 3: First multi-tasking QSAR model for Input-Coded prediction, structural back-projection, and complex networks clustering of antiprotozoal compounds. *Bioorg. Med. Chem.* **2008**, *16*, 5871–5880. (j) Wang, X. S.; Tang, H.; Golbraikh, A.; Tropsha, A. Combinatorial QSAR modeling of specificity and subtype selectivity of ligands binding to serotonin receptors 5HT1E and 5HT1F. *J. Chem. Inf. Model.* **2008**, *48* (5), 997–1013. (k) Dea-Ayuela, M. A.; Perez-Castillo, Y.; Meneses-Marcel, A.; Ubeira, F. M.; Bolas-Fernandez, F.; Chou, K. C.; Gonzalez-Diaz, H. HP-Lattice QSAR for dynein proteins: Experimental proteomics (2D-electrophoresis, mass spectrometry) and theoretic study of a Leishmania infantum sequence. *Bioorg. Med. Chem.* **2008**, *16*, 7770–7776. (l) Du, Q. S.; Huang, R. B.; Chou, K. C. Recent advances in QSAR and their applications in predicting the activities of chemical molecules, peptides and proteins for drug design. *Curr. Protein Pept. Sci.* **2008**, *9*, 248–259. (m) Gonzalez-Díaz, H.; Gonzalez-Díaz, Y.; Santana, L.; Ubeira, F. M.; Uriarte, E. Proteomics, networks, and connectivity indices. *Proteomics* **2008**, *8*, 750–778. (n) Costanzi, S.; Tikhonova, I. G.; Harden, T. K.; Jacobson, K. A. Ligand and structure-based methodologies for the prediction of the activity of G protein-coupled receptor ligands. *J. Comput.-Aided Mol. Des.* **2008**.

(32) (a) Feng, Z. P. An overview on predicting the subcellular location of a protein. *In Silico Biol.* **2002**, *2* (3), 291–303. (b) Chou, K. C.; Shen, H. B. Predicting eukaryotic protein subcellular location by fusing optimized evidence-theoretic K-nearest neighbor classifiers. *J. Proteome Res.* **2006**, *5*, 1888–1897. (c) Chou, K. C.; Shen, H. B. Hum-PLoc: A novel ensemble classifier for predicting human protein subcellular localization. *Biochem. Biophys. Res. Commun.* **2006**, *347*, 150–157. (d) Chou, K. C.; Shen, H. B. Recent progresses in protein subcellular location prediction. *Anal. Biochem.* **2007**, *370*, 1–16. (e) Chou, K. C.; Shen, H. B. Euk-mPLoc: a fusion classifier for large-scale eukaryotic protein subcellular location prediction by incorporating multiple sites. *J. Proteome Res.* **2007**, *6*, 1728–1734. (f) Chou, K. C.; Shen, H. B. Cell-PLoc: A package of web-servers for predicting subcellular localization of proteins in various organisms. *Nat. Protoc.* **2008**, *3*, 153–162.

(33) (a) Dean, M. K.; Higgs, C.; Smith, R. E.; Bywater, R. P.; Snell, C. R.; Scott, P. D.; Upton, G. J.; Howe, T. J.; Reynolds, C. A. Dimerization of G-protein-coupled receptors. *J. Med. Chem.* **2001**, *44* (26), 4595–614. (b) Cavasotto, C. N.; Orry, A. J.; Abagyan, R. A. Structure-based identification of binding sites, native ligands and potential inhibitors for G-protein coupled receptors. *Proteins* **2003**, *51* (3), 423–33. (c) Verdonk, E.; Johnson, K.; McGuinness, R.; Leung, G.; Chen, Y. W.; Tang, H. R.; Michelotti, J. M.; Liu, V. F. Cellular dielectric spectroscopy: a label-free comprehensive platform for functional evaluation of endogenous receptors. *Assay Drug Dev. Technol.* **2006**, *4* (5), 609–19. (d) Chou, K. C.; Shen, H. B. MemType-2L: A Web server for predicting membrane proteins and their types by incorporating evolution information through Pse-PSSM. *Biochem. Biophys. Res. Commun.* **2007**, *360*, 339–345.

(34) (a) Maurin, C.; Bailly, F.; Cotelle, P. Structure-activity relationships of HIV-1 integrase inhibitors--enzyme-ligand interactions. *Curr. Med. Chem.* **2003**, *10* (18), 1795–810. (b) Kuznetsova, E.; Proudfoot, M.; Sanders, S. A.; Reinking, J.; Savchenko, A.; Arrowsmith, C. H.; Edwards, A. M.; Yakunin, A. F. Enzyme genomics: Application of general enzymatic screens to discover new enzymes. *FEMS Microbiol. Rev.* **2005**, *29* (2), 263–79. (c) Shen, H. B.; Chou, K. C. EzyPred: A top-down approach for predicting enzyme functional classes and subclasses. *Biochem. Biophys. Res. Commun.* **2007**, *364*, 53–59. (d) Bartlam, M.; Xu, Y.; Rao, Z. Structural proteomics of the SARS coronavirus: a model response to emerging infectious diseases. *J. Struct. Funct. Genomics* **2007**, *8* (2−3), 85–97. (e) Margis, R.; Dunand, C.; TeixeiraF. K.; Margis-Pinheiro, M. Glutathione peroxidase family - an evolutionary overview. *FEBS J.* **2008**, *275* (15), 3959–70.

(35) (a) Chou, K. C.; Elrod, D. W. Bioinformatical analysis of G-protein-coupled receptors. *J. Proteome Res.* **2002**, *1*, 429–433. (b) Parmigiani, R. B.; Magalhães, G. S.; Galante, P. A.; Manzini, C. V.; Camargo, A. A.; Malnic, B. A novel human G protein-coupled receptor is over-expressed in prostate cancer. *Genet. Mol. Res.* **2004**, *3* (4), 521–31. (c) Chou, K. C. Prediction of G-protein-coupled receptor classes. *J. Proteome Res.* **2005**, *4*, 1413–1418. (d) Verdonk, E.; Johnson, K.; McGuinness, R.; Leung, G.; Chen, Y. W.; Tang, H. R.; Michelotti, J. M.; Liu, V. F. Cellular dielectric spectroscopy: a label-free comprehensive platform for functional evaluation of endogenous receptors. *Assay Drug Dev. Technol.* **2006**, *4* (5), 609–19.

(36) (a) Mannello, F. Natural bio-drugs as matrix metalloproteinase inhibitors: new perspectives on the horizon. *Recent Pat. Anti-Cancer Drug Discovery* **2006**, *1* (1), 91–103. (b) Calzado, M. A.; Bacher, S.; Schmitz, M. L. NF-kappaB inhibitors for the treatment of inflammatory diseases and cancer. *Curr. Med. Chem.* **2007**, *14* (3), 367–76. (c) Chou, K. C.; Shen, H. B. ProtIdent: A web server for identifying proteases and their types by fusing functional domain and sequential evolution information. *Biochem. Biophys. Res. Commun.* **2008**, *376*, 321–325.

(37) (a) Senior, A. E. Catalytic sites of Escherichia coli F1-ATPase. *J. Bioenerg. Biomembr.* **1992**, *24* (5), 479–84. (b) Chou, K. C. A vectorized sequence-coupling model for predicting HIV protease cleavage sites in proteins. *J. Biol. Chem.* **1993**, *268*, 16938–16948. (c) Chou, K. C. Prediction of HIV protease cleavage sites in proteins. *Anal. Biochem.* **1996**, *233*, 1–14. (d) Lohmüller, T.; Wenzler, D.; Hagemann, S.; Kiess, W.; Peters, C.; Dandekar, T.; Reinheckel, T. Toward computer-based cleavage site prediction of cysteine endopeptidases. *Biol. Chem.* **2003**, *384* (6), 899–909. (e) Yang, Z. R.; Hamer, R. Bio-basis function neural networks in protein data mining. *Curr. Pharm. Des.* **2007**, *13* (14), 1403–13. (f) Shen, H. B.; Chou, K. C. HIVcleave: a web-server for predicting HIV protease cleavage sites in proteins. *Anal. Biochem.* **2008**, *375*, 388–390.

(38) (a) Luca, S.; White, J. F.; Sohal, A. K.; Filippov, D. V.; van Boom, J. H.; Grisshammer, R.; Baldus, M. The conformation of neurotensin bound to its G protein-coupled receptor. *Proc. Natl. Acad. Sci. U.S.A.* **2003**, *100* (19), 10706–11. (b) Fariselli, P.; Finelli, M.; Rossi, I.; Amico, M.; Zauli, A.; Martelli, P. L.; Casadio, R. TRAMPLE: the transmembrane protein labelling environment. *Nucleic Acids Res.* **2005**, *33*. (c) Nemoto, W.; Toh, H. Membrane interactive alpha-helices in GPCRs as a novel drug target. *Curr. Protein Pept. Sci.* **2006**, *7* (6), 561–75. (d) Chou, K. C.; Shen, H. B. Signal-CF: a subsite-coupled and window-fusing approach for predicting signal peptides. *Biochem. Biophys. Res. Commun.* **2007**, *357*, 633–640. (e) Shen, H. B.; Chou, K. C. Signal-3L: a 3-layer approach for predicting signal peptide. *Biochem. Biophys. Res. Commun.* **2007**, *363*, 297–303.

(39) (a) Okada, T.; Le Trong, I.; Fox, B. A.; Behnke, C. A.; Stenkamp, R. E.; Palczewski, K. X-Ray diffraction analysis of three-dimensional crystals of bovine rhodopsin obtained from mixed micelles. *J. Struct. Biol.* **2000**, *130*, 73–80. (b) Palczewski, K.; Kumasaka, T.; Hori, T.; Behnke, C. A.; Motoshima, H.; Fox, B. A.; Le Trong, I.; Teller, D. C.; Okada, T.; Stenkamp, R. E.; Yamamoto, M.; Miyano, M. Crystal Structure of Rhodopsin: A G Protein-Coupled Receptor. *Science* **2000**, *289*, 739–745. (c) Teller, D. C.; Okada, T.; Behnke, C. A.; Palczewski, K.; Stenkamp, R. E. Advances in determination of a high-resolution three-dimensional structure of rhodopsin, a model of G-protein-coupled receptors (GPCRs). *Biochemistry* **2001**, *40*, 7761–72. (d) Okada, T.; Palczewski, K. Crystal structure of rhodopsin: implications for vision and beyond. *Curr. Opin. Struct. Biol.* **2001**, *11*, 420–6. (e) Ballesteros, J. A.; Palczewski, K. G protein-coupled receptor drug discovery: implications from the crystal structure of rhodopsin. *Curr. Opin. Drug Discovery Dev.* **2001**, *4*, 561–74. (f) Stenkamp, R. E.; Teller, D. C.; Palczewski, K. Crystal structure of rhodopsin: a G-protein-coupled receptor. *ChemBioChem* **2002**, *3*, 963–7. (g) Filipek, S.; Teller, D. C.; Palczewski, K.; Stenkamp, R. The crystallographic model of rhodopsin and its use in studies of other G protein-coupled receptors. *Annu. Rev. Biophys. Biomol. Struct.* **2003**, *32*, 375–97. (h) Salom, D.; Le Trong, I.; Pohl, E.; Ballesteros, J. A.; Stenkamp, R. E.; Palczewski, K.; Lodowski, D. T. Improvements in G protein-coupled receptor purification yield light stable rhodopsin crystals. *J. Struct. Biol.* **2006**, *156*, 497–504. (i) Salom, D.; Lodowski, D. T.; Stenkamp, R. E.; Le Trong, I.; Golczak, M.; Jastrzebska, B.; Harris, T.; Ballesteros, J. A.; Palczewski, K. Crystal structure of a photoactivated deprotonated intermediate of rhodopsin. *Proc. Natl. Acad. Sci. U.S.A.* **2006**, *103*, 16123–8.

(40) (a) Chaturvedi, K.; Christoffers, K. H.; Singh, K.; Howells, R. D. Structure and regulation of opioid receptors. *Biopolymers* **2000**, *55*, 334–46. (b) Ballesteros, J. A.; Shi, L.; Javitch, J. A. Structural mimicry in G protein-coupled receptors: implications of the high-resolution structure of rhodopsin for structure-function analysis of rhodopsin-like receptors. *Mol. Pharmacol.* **2001**, *60*, 1–19. (c) Becker, O. M.; Shacham, S.; Marantz, Y.; Noiman, S. Modeling the 3D structure of GPCRs: advances and application to drug discovery. *Curr. Opin. Drug Discovery Dev.* **2003**, *6*, 353–61. (d) Moro, S.; Spalluto, G.; Jacobson, K. A. Techniques: Recent developments in computer-aided engineering of GPCR ligands using the human adenosine A3 receptor as an example. *Trends Pharmacol. Sci.* **2005**, *26*, 44–51. (e) Zhang, Y.; Sham, Y. Y.; Rajamani, R.; Gao, J.; Portoghese, P. S. Homology modeling and molecular dynamics simulations of the mu opioid receptor in a membrane-aqueous system. *ChemBioChem* **2005**, *6*, 853–9. (f) Nowak, M.; Kolaczkowski, M.; Pawlowski, M.; Bojarski, A. J. Homology modeling of the serotonin 5-HT_1A receptor using automated docking of bioactive compounds with defined geometry. *J. Med. Chem.* **2006**, *49*, 205–14. (g) McLean, T. H.; Chambers, J. J.; Parrish, J. C.; Braden, M. R.; Marona-Lewicka, D.; Kurrasch-Orbaugh, D.; Nichols, D. E. C-(4,5,6-trimethoxyindan-1-yl)methanamine: a mescaline analogue designed using a homology model of the 5-HT_2A receptor. *J. Med. Chem.* **2006**, *49*, 4269–74. (h) Hobrath, J. V.; Wang, S. Computational elucidation of the structural basis of ligand binding to the dopamine 3 receptor through docking and homology modeling. *J. Med. Chem.* **2006**, *49*, 4470–6. (i) Patny, A.; Desai, P. V.; Avery, M. A. Homology modeling of G-protein-coupled receptors and implications in drug design. *Curr. Med. Chem.* **2006**, *13*, 1667–91. (j) Singh, S.; Malik, B. K.; Sharma, D. K. Targeting HIV-1 Through Molecular Modeling and Docking Studies of CXCR4: Leads for Therapeutic Development. *Chem. Biol. Drug Des.* **2007**, *69*, 191–203.

(41) Patny, A.; Desai, P. V.; Avery, M. A. Ligand-supported homology modeling of the human angiotensin II type 1 (AT(1)) receptor: insights into the molecular determinants of telmisartan binding. *Proteins* **2006**, *65*, 824–42.

(42) Lu, Z. L.; Saldanha, J. W.; Hulme, E. C. Seven-transmembrane receptors: crystals clarify. *Trends Pharmacol. Sci.* **2002**, *23*, 140–6.

(43) (a) Cherezov, V.; Rosenbaum, D. M.; Hanson, M. A.; Rasmussen, S. G.; Thian, F. S.; Kobilka, T. S.; Choi, H. J.; Kuhn, P.; Weis, W. I.; Kobilka, B. K.; Stevens, R. C. High-Resolution Crystal Structure of an Engineered Human (beta)2-Adrenergic G Protein-Coupled Receptor. *Science* **2007**, *318*, 1258–65. (b) Rosenbaum, D. M.; Cherezov, V.; Hanson, M. A.; Rasmussen, S. G.; Thian, F. S.; Kobilka, T. S.; Choi, H. J.; Yao, X. J.; Weis, W. I.; Stevens, R. C.; Kobilka, B. K. GPCR Engineering Yields High-Resolution Structural Insights into (beta)2 Adrenergic Receptor Function. *Science* **2007**, *318*, 1266–73. (c) Rasmussen, S. G.; Choi, H. J.; Rosenbaum, D. M; Kobilka, T. S; Thian, F. S.; Edwards, P. C.; Burghammer, M. V. R; Ratnala, R.; Sanishvili, R. F.; Fischetti, G. F; Schertler, W. I.; Weis, B. K.; Kobilka, *Nature* **2007**, *450*, 383–7.

(44) (a) Kobilka, B.; Schertler, G. F. New G-protein-coupled receptor crystal structures: insights and limitations. *Trends Pharmacol. Sci.* **2008**, *29* (2), 79–83. (b) Lefkowitz, R. J.; Sun, J. P.; Shukla, A. K. A crystal clear view of the beta2-adrenergic receptor. *Nat. Biotechnol.* **2008**, *26* (2), 189–91. (c) Shukla, A. K.; Sun, J. P.; Lefkowitz, R. J. Crystallizing thinking about the beta2-adrenergic receptor. *Mol. Pharmacol.* **2008**, *73* (5), 1333–8. (d) Costanzi, S. On the applicability of GPCR homology models to computeraided drug discovery: a comparison between in silico and crystal structures of the beta2-adrenergic receptor. *J. Med. Chem.* **2008**, *51* (10), 2907–14.

(45) Laskowski, R. A.; MacArthur, M. W.; Moss, D. S.; Thornton, J. M. Procheck—a program to check the stereochemical quality of protein structures. *J. Appl. Crystallogr.* **1993**, *26*, 283–291.

(46) Dragic, T.; Trkola, A.; Lin, S. W.; Nagashima, K. A.; Kajumo, F.; Zhao, L.; Olson, W. C.; Wu, L.; Mackay, C. R.; Allaway, G. P.; Sakmar, T. P.; Moore, J. P.; Maddon, P. J. Amino-Terminal Substitutions in the CCR5 Coreceptor Impair gp120 Binding and Human Immunodeficiency Virus Type 1 Entry. *J. Virol.* **1998**, *72*, 279–285.

(47) Farzan, M.; Choe, H.; Vaca, L.; Martin, K.; Sun, Y.; Desjardins, E.; Ruffing, N.; Wu, L.; Wyatt, R.; Gerard, N.; Gerard, C.; Sodroski, J. A Tyrosine-Rich Region in the N Terminus of CCR5 Is Important for Human Immunodeficiency Virus Type 1 Entry and Mediates an Association between gp120 and CCR5. *J. Virol.* **1998**, *72*, 1160–1164.

(48) Rabut, G. E. E.; Konner, J. A.; Kajumo, F.; Moore, J. P.; Dragic, T. Alanine Substitutions of Polar and Nonpolar Residues in the Amino-Terminal Domain of CCR5 Differently Impair Entry of Macrophage- and Dualtropic Isolates of Human Immunodeficiency Virus Type 1. *J. Virol.* **1998**, *72*, 3464–3468.

(49) Cormier, E. G.; Persuh, M.; Thompson, D. A. D.; Lin, S. W.; Sakmar, T. P.; Olson, W. C.; Dragic, T. Specific interaction of CCR5 amino-terminal domain peptides containing sulfotyrosines with HIV-1 envelope glycoprotein gp120. *Proc. Natl. Acad. Sci. U.S.A.* **2000**, *97*, 5762–5767.

(50) Genoud, S.; Kajumo, F.; Guo, Y.; Thompson, D.; Dragic, T. CCR5-Mediated Human Immunodeficiency Virus Entry Depends on an Amino-Terminal gp120-Binding Site and on the Conformational Integrity of All Four Extracellular Domains. *J. Virol.* **1999**, *73*, 21645–1648.

(51) Siciliano, S. J.; Kuhmann, S. E.; Weng, Y.; Madani, N.; Springer, M. S.; Lineberger, J. E.; Danzeisen, R.; Miller, M. D.; Kavanaugh, M. P.; DeMartino, J. A.; Kabat, D. A. A Critical Site in the Core of the CCR5 Chemokine Receptor Required for Binding and Infectivity of Human Immunodeficiency Virus Type 1. *J. Biol. Chem.* **1999**, *274*, 1905–1913.

(52) Chabot, D. J.; Broder, C. C. Substitutions in a Homologous Region of Extracellular Loop 2 of CXCR4 and CCR5 Alter Coreceptor Activities for HIV-1 Membrane Fusion and Virus Entry. *J. Biol. Chem.* **2000**, *275*, 23774–23782.

(53) Blanpain, C.; Doranz, B. J.; Bondue, A.; Govaerts, C.; De Leener, A.; Vassart, G.; Doms, R. W.; Proudfoot, A.; Parmentier, M. The Core Domain of Chemokines Binds CCR5 Extracellular Domains while Their Amino Terminus Interacts with the Transmembrane Helix Bundle. *J. Biol. Chem.* **2003**, *278*, 5179–5187.

(54) Zhou, N.; Luo, Z.; Hall, J. W.; Luo, J.; Han, X.; Huang, Z. Molecular modeling and site-directed mutagenesis of CCR5 reveal residues critical for chemokine binding and signal transduction. *Eur. J. Immunol.* **2000**, *30*, 164–73.
(55) (a) Jones, G.; Willett, P.; Glen, R. C. ; Molecular recognition of receptor sites using a genetic algorithm with a description of desolvation. *J. Mol. Biol.* **1995**, *245*, 43–53. (b) Jones, G.; Willett, P.; Glen, R. C.; Leach, A. R.; Taylor, R. Development and Validation of a Genetic Algorithm for Flexible Docking. *J. Mol. Biol.* **1997**, *267*, 727–748.

CI800356A